Investigation of the Kinematics and Kinetics of Whiplash

H. J. Mertz, Jr. and L. M. Patrick Wayne State University

Abstract

The kinematics of rear-end collisions based on published acceleration pulses of actual car-to-car collisions (10 and 23 mph) were reproduced on a crash simulator using anthropomorphic dummies, human cadavers, and a volunteer. Comparison of the responses of subjects without head support were based on the reactions developed at the base of the skull (occipital condyles). The cadavers gave responses which were representative of persons unaware of an impending collision. The responses of both dummies used were not comparable with those of the cadavers or volunteer, or to each other.

An index based on voluntary human tolerance limits to statically applied head loads was developed and used to determine the severity of the simulations for the unsupported head cases. Results indicated that head torque rather than neck shear or axial forces is the major factor in producing neck injury.

When the head was initially supported by a flat, padded headrest, all subjects gave comparable headrest loads. Using this configuration, the volunteer withstood an equivalent 44 mph simulation with only slight discomfort.

With the head separated from the headrest by 2-3/4 in. the head load increased from 150 to 390 lb, but with additional padding, the load was increased to only 250 lb.

Controlled seat back rotation decreased the magnitudes of the head loads and neck reactions for the supported and unsupported head cases, respectively.

THE SO-CALLED WHIPLASH SYNDROME constitutes the most prevalent trauma to occupants of automobiles struck from the rear. It is particularly insidious with subtle pathology that often does not show up with radiological or other quantitative diagnostic techniques. Acute or chronic symptoms sometimes persist for years, and in some cases where there is no immediate obvious morbidity, injuries attributed to the accident show up months later. Fortunately, whiplash is seldom disabling during the recovery period, and it is generally amenable to conservative treatment. Some orthopedic surgeons advocate operative procedures only after 2 years of other types of treatment are unsuccessful. Lesions ranging from vague aches, pains, vertigo, and dysphagia to torn muscles, ligament damage, joint injuries, and bone damage have been reported by physicians. Experiments have reproduced some of the lesions in laboratory animals and human cadavers with various types of sleds and accelerators. However, the mechanics of whiplash are not well known, and the

correlation of animals, cadavers, and living human beings is not accurately established.

Many mechanisms for explaining injuries associated with acceleration hyperextension have been postulated. The most obvious is one in which the neck is treated as a beam in bending with posterior compression injuries to the cervical vertebrae and/or to the intervertebral discs. Tensile forces due to bending produce anterior tissue damage. While these injuries have been observed clinically and experimentally, tension-type lesions to the soft tissue at the back of the neck have also been found.

Tensile damage to the soft tissue at the back of the neck has led to the theory that the injury in the whiplash accident results not during the hyperextension portion of the cycle but, instead, on the flexion rebound portion. This explains the torn tissues at the back of the neck but is hard to justify due to the difficulty in reproducing this type of injury in the laboratory and also due to the fact that the chin provides a mechanical stop or limitation to the flexion as it strikes the chest. When the chin strikes the chest, the back of the neck will still be in tension but the stresses would be expected to be below those producing injury due to the large moment arm from the chin to back of the neck.

It has been hypothesized that injury occurs during the initial part of the acceleration cycle from shear action caused by a presumed relative motion between the head and torso prior to appreciable rotation. If this theory is correct, the head support proposed as a means of eliminating the acceleration-extension injury would have to be against the head at all times with little or no padding for comfort.

The general purpose of this research program is to establish the actual injury mechanism, while the detailed objectives are to:

- 1. Analyze forces and moments at the base of the skull during acceleration extension.
 - 2. Verify the analysis experimentally.
- 3. Compare the experimental results of anthropomorphic dummies, cadavers, and human volunteers.
 - 4. Study the effectiveness of head support in mitigating whiplash injury.
- 5. Determine the effect of seat back rotation on acceleration-extension parameters.
 - 6. Correlate human voluntary static forces and moments with impact severity.

Using the comparison of the results from anthropomorphic dummy and cadaver impacts with those from the human volunteer as a basis, a logical extrapolation from the subinjury to the injury impact severity is expected to be achieved in future work. The present program includes only two degrees of severity (severe and nonsevere) which were simulated from data of actual car-to-car collisions published by Severy and Mathewson (1)!

Voluntary Human Neck Tolerances to Statically Applied Head Loads

Basis for Static Tolerance Level - Analyzing the head as a free body (Fig. 1), the important parameters are the reactions at the base of the skull. These reactions must accelerate the head during whiplash and consequently cause the neck to hyperextend. Since the motion is two dimensional, these reactions can be resolved into a shear force

¹Numbers in parentheses designate References at end of paper.

 R_{811} acting perpendicular to the vertebral column at the occipital condyles and lying in the mid-sagittal plane, an axial force R_{812} acting along the axis of the second cervical vertebra, and a resulting couple T_8 acting about an axis passing through the point of intersection of the shear and axial forces and perpendicular to the mid-sagittal plane.

Maximum tolerable static limits for these reactions were determined for various loading configurations and serve as a basis for voluntary neck tolerances to statically applied head loads.

Procedure - Five different static loading configurations were investigated using the same volunteer who was also subjected to the simulated whiplash environment. In the first four configurations the subject was strapped in a seated position in a rigid chair. The loads were applied by the volunteer using a block and tackle arrangement shown in Fig. 2 and were transferred to the head through a tightly fitted plastic headband from a welding visor. An axial load cell inserted between the block and tackle and the headband sensed the applied load.

In the fifth configuration the volunteer assumed a standing position with his head supported in the occipital and mandible regions by a cradle constructed of seat belt webbing material. The cradle was fastened to a load cell which was secured to the ceiling. Load was applied to the neck by the weight of the subject with additional force being applied by the subject pulling up against a fixed horizontal bar.

The instrumentation was the same for the five configurations. The load was measured by a strain gage axial sensitive load cell whose output was recorded continuously on light-sensitive paper by a light beam galvanometer. Direction and point of application of the load were recorded incrementally using a 35 mm SLR Nikon camera equipped with a battery powered shutter firing and film advance system. The shutter pulse was recorded on the light-sensitive paper to give a time correlation between the photograph and the applied load.

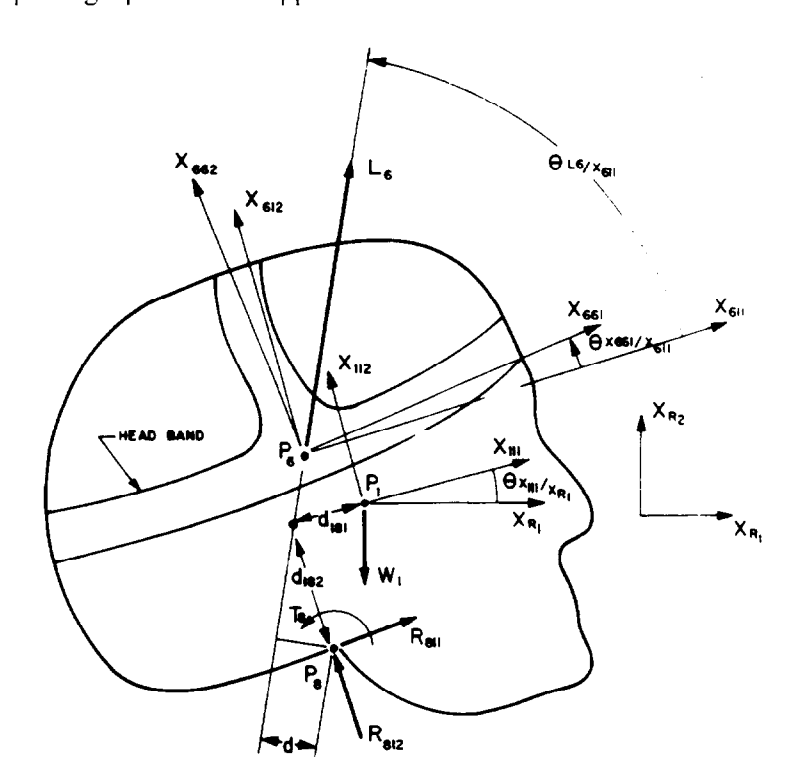


Fig. 1 — Free body diagram of statically loaded head

Method of Data Reduction — The neck reactions for all configurations were computed by considering the head as a free body (Fig. 1). Four orthogonal coordinate systems were assumed. The $(X_R)_i$ set was chosen as an absolute system with X_{R_1} axis being horizontal with respect to the ground. The (X_{66}) i system was assumed fixed to the head with the origin P_6 at the point of application of the applied load with the X_{661} axis parallel to the superior edge of the circumferential part of the headband. The $(X_{61})_i$ system rotated with the head, with the origin also taken at point P_6 . However, the X_{611} axis was directed in a posterior to anterior (P-A) direction parallel to the direction of the shear reaction at the base of the skull, and the X_{612} axis was directed in an inferior to superior (I-S) direction. The fourth system $(X_{11})_i$ was affixed to the skull at P_1 , the center of gravity of the head. The X_{111} axis was oriented in the P-A direction with the X_{112} axis superiorly directed. Point P_8 was taken at the occipital condyles and had to be approximated from surface landmarks of the side of the face. To determine the reactions at P_8 , the equations of static equilibrium were applied:

$$\Sigma \mathbf{F}_{611} = 0 \tag{1a}$$

$$\Sigma F_{612} = 0 \tag{1b}$$

$$\Sigma M_8 = 0 \tag{1c}$$

Resolving the applied load, L_6 , and the head weight, W_1 , into components and substituting these values into Eq. 1, the following expressions for neck reactions are obtained:

$$R_{811} = W_1 \sin(\theta_{X_{111}/X_{R_1}}) - L_6 \cos(\theta_{L_6/X_{611}})$$
 (2a)

$$R_{812} = W_1 \cos(\theta_{X_{111}/X_{R_1}}) - L_6 \sin(\theta_{L_6/X_{611}})$$
 (2b)

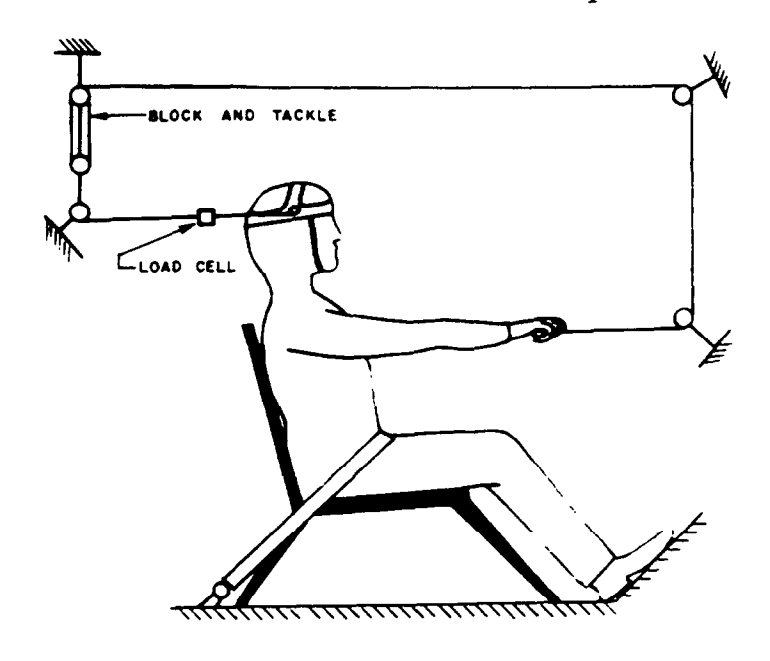


Fig. 2 — Setup for applying static head loads

where

$\theta_{X_{111/X_{R_1}}}$

Angle between X_{111} coordinate axis and the horizontal $\theta_{L_6/X_{611}}$

Angle between L₆ and X₆₁₁ axis

The magnitude of the resulting torque is given by

$$T_8 = L_6(d) + W_1 \cos(\theta_{X_{111}/X_{R_1}}) d_{181} - W_1 \sin(\theta_{X_{111}/X_{R_1}}) d_{182}$$
 (3)

Table 1 — Maximum Reactions for Various Static Loading Configurations (Volunteer - LMP, $W_1 = 10.8$ lb, $d_{181} = 0.75$ in., $d_{182} = 2.44$ in.)

			•	101	102		
Run	Configuration ^a	^L 6,	Θ _{L 6/} 811,	Θ _{X111/} X _{R1}	^R 811, Ib	Max. Value R _{812,} lb	T _{8,}
		lb	deg	deg			
S-1	1	34	187	1	33.7	14.9	- 9.1
S-1	1	34	192	- 3	33.3	17.9	- 8.1
S-2	1	41	196	- 8	39.5	21.8	-10.1
S-2	1	40	191	- 3	39.2	18.4	-10.6
S-4	2	64	205	-18	55.0	36.9	-12.7
S- 4	2	61	207	-21	54.4	37.8	-10.4
S -5	2	64	201	-17	56.6	33.7	-10.8
S-6	3	68	159	25	68.1	-14.5	-17.5
5.7 b	3	41	123	64	32.0	-29.6	- 7.3
S-8 ^c	3	89	75	82	-12.7	-86.2	-14.5
S- 8	3	63	82	75	1.7	-62.5	-14.6
S- 9	4	164	•	*	*	*	*
S-10	4	148	*	*	*	*	•
S-11	4	175	*	*	•	*	*
S-12	5	330	53	36	-192.0	-254.0	0

^{*} Not measured.

^a Configuration 1 - Head in normal position, load A-P.

^{2 -} Head in flexed position, load A-P.

^{3 -} Head in extended position, load A-P.

^{4 -} Bracing head with hands, load A-P.

^{5 -} Hanging position.

^b Headband digging into forehead.

^cRubber inserted between headband and forehead.

To solve these equations for the neck reactions, the magnitudes of the applied loads were obtained from the light beam oscillograph records and the geometric parameters were measured from the corresponding photographs. The positive directions of these results are shown on the free body diagram.

Results and Discussion — The resulting maximum reactions for the five configurations which were evaluated are presented in Table 1.

For the first configuration (runs S-1 and S-2), the head was held upright in a normal position. The load was applied essentially in the A-P (anterior to posterior) direction as indicated by the angle $O_{L_0}/X_{\rm en}$. The maximum torque which could be resisted by the neck muscles before the head began to rotate was -10.6 ft-lb; the maximum shear load developed during this loading sequence was 39.5 lb. The axial load is of no significance, since the principal load was not in this direction.

In the second configuration (runs S-4 and S-5), the head was flexed forward from its normal position, causing the applied load to place a compressive load on the neck vertebrae. In this position the mechanical advantages of the neck muscles which limit extension of the neck have increased, resulting in a higher maximum resistive neck torque (- 12.7 ft-lb) than was obtained when the head was held upright. Also, for this configuration the maximum shear load and compressive axial loads were increased to 56.6 and 37.8 lb, respectively.

The advantages of this head position compared to the normal upright position in a rear-end collision are twofold:

- 1. The neck torque has been increased from -10.6 to -12.7 ft-lb, which implies that a more severe impact can be withstood.
- 2. The angle through which the head would rotate before severe hyperextension occurs would be greater, resulting in more energy being dissipated during the rotation, which would reduce the degree of hyperextension.

In the third configuration the head was rotated rearward from a normal upright position with load being applied in an A-P, S-I direction. In this position the maximum neck torque was increased to -17.5 ft-lb. This increase was primarily due to a change in the point of rotation of the head with respect to the neck. Instead of rotating about the condyles at the base of the skull, the head rotates about the posterior portion of the first cervical vertebra. Consequently, the effective moment arm of the neck muscles, which restrict this rotation, has been increased, resulting in a larger resistive neck couple for a given resultant muscle force. Also, the anterior ligaments of the neck vertebrae are elongated, resulting in additional load-carrying capacity. The maximum measured shear and axial tension forces were 68.1 and -86.2 lb, respectively.

On a comparative basis, this configuration gives a higher resistive neck torque level than the previous two, which implies that the volunteer could withstand a more severe rear-end collision in this position.

Configuration 4 was evaluated to determine a suitable position which a person could assume if he is aware of an impending rear-end collision. In this configuration the volunteer grasped his hands together behind his head, providing support against head rotation with his arms. The load was applied in an A-P direction and his head remained in a normal upright position. The maximum applied load was 175 lb as compared to maximum applied loads of 41, 64, and 89 lb for the unsupported normal, flexed, and extended positions of the head, respectively. Consequently, this con-

figuration offers the greatest degree of safety against hyperextension of the head. Further increase in safety could be accomplished by using this method with the head initially bent forward.

To determine the strength of the neck in tension, the volunteer was subjected to a hanging type of loading in configuration 5. In this position a maximum axial tension load of -254 lb was achieved. The corresponding shear load was -192 lb.

Additional voluntary human tolerance levels applied to the reactions at the base of the skull can be obtained by modifying other researchers' published results. Since the method of modifying these results may be doubtful, an explanation of the assumptions and calculations used in each modification follows.

From a paper presented by Stapp (2) it was stated that an "upward seat ejection safe limit" was 20 g. Assuming an average weight of a head of 12 lb, a 20 g acceleration of the head would require an axial compressive force at the base of the skull of 240 lb. This value is probably on the low side, since a pilot would be wearing a helmet which would increase the weight of the head. Taking into account this additional assumption, a voluntary neck axial compressive force of 250 lb should not be injurious.

In a paper by Carroll, et al. (3), five human volunteers were subjected to static and dynamic P-A head loads with the head being initially in a normal upright position. The load was applied through a headband which was positioned 1/2 in. superiorly to the occipital prominence. Their results indicated that an average static "neck torque" of 40.7 ft-lb could be developed. Through personal communication it was learned that the point of rotation for computing these torques was taken as the mid-clavicle, resulting in a range of moment arms of 7-7-1/2 in. The average distance from the midclavicle to the midpoint of the external auditory canal was 5-1/8 in. Since the torques developed at the occipital condyles are needed to compare with the results obtained using volunteer LMP, the torques given by Carroll, et al. were recalculated. Based on a moment arm of 7-1/4 in., the average 40.7 ft-lb moment was produced by applying a 67.3 lb force. Assuming that the distance from the applied load to the occipital condyle is 2-3/4 in., a resulting couple and shear force at the base of the skull of 15.4 ft-lb and -67.3 lb, respectively, are needed to maintain equilibrium. The difference between this torque (15.4 ft-lb with the load applied in the P-A direction) and the maximum torque (-10.6 ft-1b with the load applied in the A-P direction) is not as great as expected, since the largest neck muscles are attached to the skull in the occipital region, which implies that a person should be able to resist much larger flexual torques than extending torques. Consequently, the average value given by Carroll, et al. is more conservative than those obtained from the volunteer LMP. In order to compare the two results, the maximum static neck torque of 49.5 ft-lb withstood by one of the five volunteers used by Carroll, et al. will be used. Relating this torque to the reactions at the occipital condyles gives values of 18.8 ft-lb and -82lb for the neck torque and shear force, respectively.

A rough estimate of the breaking strength of the neck is given by Simmons and Herting (4). From an eye witness report of three executions (by hanging) of criminals in Japan in which two of the three died by strangulation instead of broken necks, an approximation for the hanging force based on energy relationships was made. It was concluded that the adult human neck is capable of withstanding an applied hanging force of 2000 lb.

Using the maximum resistive forces and moments from the various sources presented, preliminary voluntary static human tolerance levels for reactions at the base of the skull can be established and are summarized in Table 2. On an average these values are certainly lower bounds to an injury tolerance level.

It should be noted that none of the P-A shear loads represent true maximums since in the configurations used, the neck torques limited the application of higher shear loads. Also, because of the torque limitation, the listed values of the A-P shear load for the normally positioned head and of the I-S axial load for the flexed head are not maximums.

Since the emphasis was on obtaining tolerance levels pertinent to hyperextension of the neck, values were not obtained for all possible combinations of head position and neck reactions. An important omission is the value for the maximum positive couple with the head fully flexed. This couple is of significance in the evaluation of upper torso restraint systems for frontal impacts.

The majority of the values presented in this table are based on only one volunteer. Data from additional volunteers are needed to verify the various tolerance levels.

Taking into account these limitations, these voluntary static human tolerance levels will be used as a basis for evaluation of the severity of neck reactions produced in dummies, cadavers, and volunteers during simulated rear-end collisions.

Simulated Rear-End Collisions

Experimental Setup - The simulated rear-end collisions were conducted on the horizontal accelerator shown in Fig. 3. The sled travels on two horizontal rails and is accelerated pneumatically with a maximum speed of 40 mph. Deceleration is accomplished by a hydraulic snubber which can be regulated to subject the sled to a rectangular or triangular deceleration pulse. The maximum deceleration is structurally limited to 25 g. The stopping distance is continuously variable up to 22 in., depending on the sled velocity.

Head Position	Shear F	orce, Ib	Axial Fa	orce, Ib	Couple, ft-lb	
	P-A	A-P	I-S	S-I	(+)	(-)
Normal	40 °	80 a,b	250 ^c		19.0 ^b	10.5
Extended	70°	190		255	• • • •	17.
Flexed	55 a		40 ^a			12.

Table 2 — Summary of Voluntary Static Human Tolerance Levels Based on Reactions Acting at the Occipital Condyles

NOTES: All values based on volunteer LMP except where noted.

Loads and torques rounded off to nearest 5 pounds and 1/2 ft-lb, respectively

Directions based on free body diagram shown in Fig. 1.

^a Value is not a maximum tolerable load.

b Based on paper by Carroll, et al. (3).

^CBased on paper by Stapp (2), a dynamic value.

The characteristics of the sled acceleration pulses for the simulations were obtained from data presented by Severy and Mathewson (1) of actual car-to-car rearend collisions. Table 3 lists the pertinent kinematic parameters for two severe and one nonsevere rear-end collisions. The changes in velocities of the struck cars were obtained by numerically integrating the curves of the longitudinal acceleration history of a point on the frame of the cars. Also, the pulse durations and peak accelerations were obtained from these curves. The g levels indicated in Table 3 could not be duplicated on the acceleration stroke of the horizontal simulator; consequently, the

Table 3 — Pertinent Kinematic Parameters from Car-to-Car Rear-End Collisions

			Struck				
Struck Car	Impact Velocity, mph	Change in Velocity, mph	Pulse Time, ms	Peak Accel., 9	Mean Accel., g	Accel. Dist., in.	
1956 Olds	10	9.1	135	5.9	3.07	10.8	
1956 Olds	23	14.8	132	10.0	5.10	17.2	
1955 Nash	23	15.2	135	10.3	5.13	18.1	

Values based on data presented by Severy and Mathewson (i). Impacting car was 1955 Hudson.

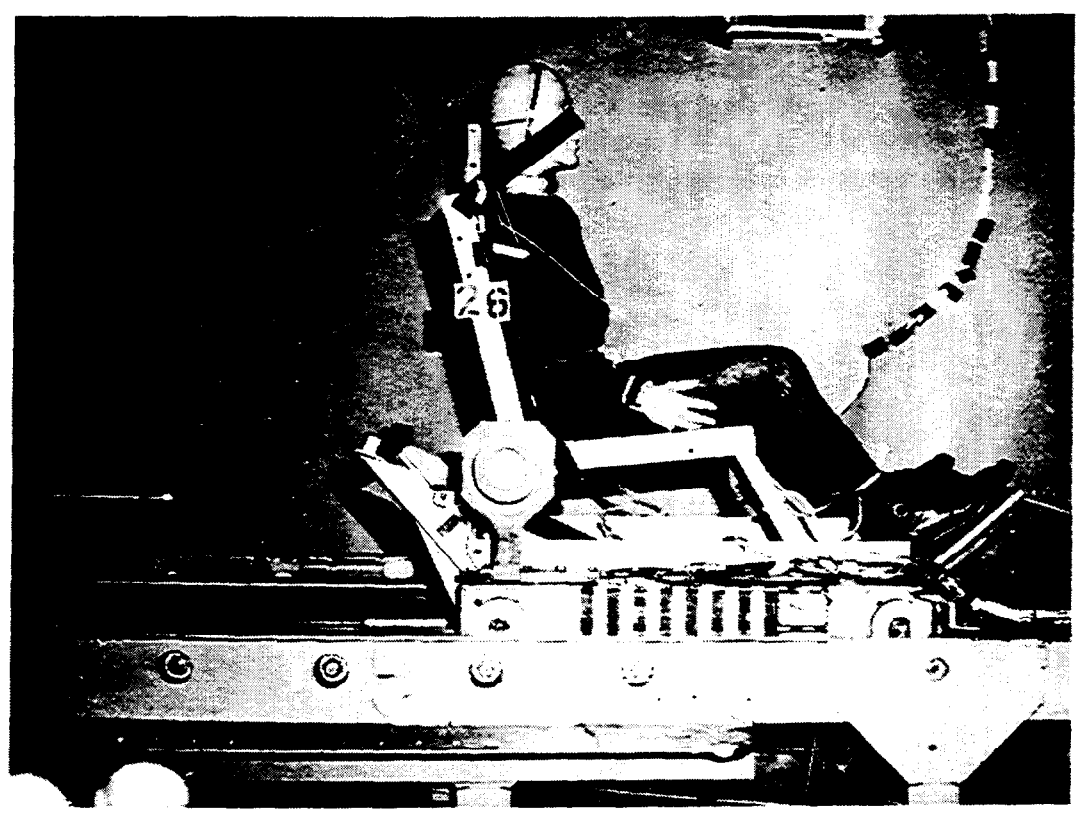


Fig. 3 — Horizontal accelerator - overall view

simulation was produced on the deceleration stroke. In order to duplicate Severy's data in this configuration, the sled velocity, stopping distance, and snubber deceleration wave shape had to be prescribed. Assuming a constant acceleration wave shape and letting the sled velocity and decelerating pulse time equal the change in velocity and acceleration-time duration of the struck car, the required stopping distance for the sled was calculated from the kinematic equations of constant acceleration. To duplicate the 10 mph, nonsevere rear-end collision, a sled velocity of 9 mph and a stopping distance of 10 in. were used. For the equivalent 23 mph, severe rear-end collision, a sled velocity of 15 mph and a stopping distance of 17.5 in. were used.

To maintain position of the subjects prior to deceleration, restraints were placed on the head, chest, and pelvic area during the acceleration stroke and were mechanically removed at the end of the stroke when the sled was moving at the prescribed constant velocity.

The seat was rigidly constructed using steel angles for main structural components and plywood coverings for the seat back and bottom. Thr rigidity of the seat back was controlled by the setting of a frictional torque limiter which allowed the seat back to rotate at prescribed levels of constant torques. The seat was mounted to the sled in a rearward facing direction. An adjustable, removable headrest was attached to the seat back.

Two types of headrest configurations, a curved and flat surface, were used. Padding to prevent localized head forces consisted of one layer of 5/8 in. Rubatex in each case. To monitor the head forces, the headrest surfaces were affixed to a biaxial load cell which was rigidly mounted to the seat back.

Determination of Neck Reactions - To evaluate the severity of the whiplash simulation and the effectiveness of the safety devices, the neck reactions and headrest loads were determined. The headrest loads were measured directly using a biaxial load cell. The neck reactions were obtained by applying the equations of dynamic equilibrium to the head. In this analysis the head is considered to be a rigid body undergoing plane motion as shown in the free body diagram (Fig. 4).

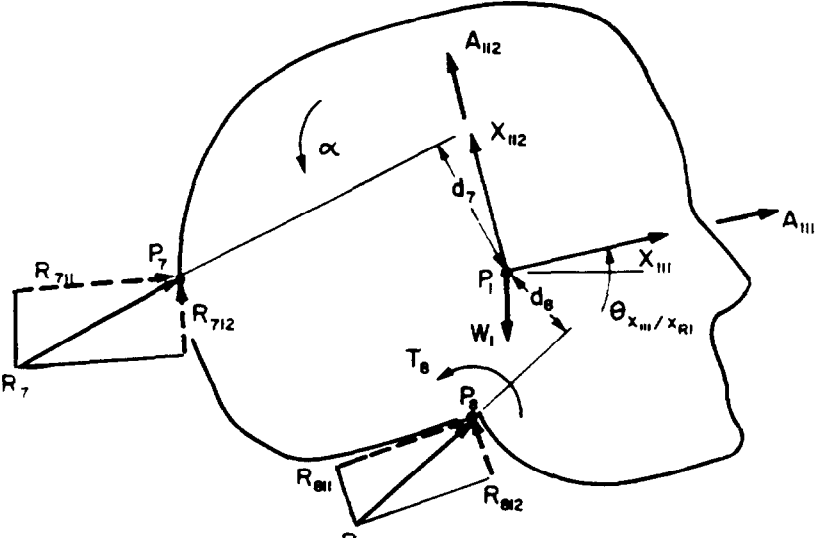


Fig. 4 — Free body diagram of head

The relevant notation is:

 P_1 = Center of gravity of the head

P₇ = Point of application of the headrest load

P₈ = Occipital condyles W₁ = Weight of head

 I_1 = Mass moment of inertia of head with respect to c.g. of head

R₈₁₁ = Shear force (described previously)
R₈₁₂ = Axial force (described previously)
R₈ = Result of the shear and axial forces
T₈ = Torque (described previously)

 R_{711} = Headrest load on head in X_{111} direction R_{712} = Headrest load on head in X_{112} direction R_7 = Result of the headrest loads R_{711} and R_{712} d_7 = Moment arm for R_7 with respect to c.g. d_8 = Moment arm for R_8 with respect to c.g.

 $\theta_{X_{111}}/X_{R_1}$ = Angle between X_{111} coordinate axis and horizontal

 α = Absolute angular acceleration of head ω = Absolute angular velocity of head

 A_{111} = Absolute acceleration of c.g. of head in X_{111} direction A_{112} = Absolute acceleration of c.g. of head in X_{112} direction

The shear reaction is given by,

$$\Sigma F_{X_{111}} = \frac{W_1}{g} A_{111}$$

or

$$R_{811} = \frac{W_1}{g} A_{111} - R_{711} + W_1 \sin \left(\theta_{X_{111}/X_{R_1}}\right)$$
 (4)

The axial force is calculated from

$$\Sigma F_{X_{112}} = \frac{W_1}{g} A_{112}$$

or

$$R_{812} = \frac{W_1}{g} A_{112} - R_{712} + W_1 \cos \left(\theta_{X_{111}/X_{R_1}}\right)$$
 (5)

And the corresponding moment, T₈, is computed from

$$\sum M_1 = I_1 \propto$$

or

$$T_8 = I_1 \propto + R_7 d_7 - R_8 d_8 \tag{6}$$

By letting $R_7 = 0$, this set of equations is valid for the case when the head is not in contact with the headrest or when the headrest is not used. The weight of the head, the mass moment of inertia, the magnitude of the headrest load, and the geometric head properties can be determined. The only parameters which must still be evaluated are the accelerations of the c.g. of the head and angular acceleration.

To obtain these parameters, the total accelerations of two points on the head were measured using biaxial accelerometers. The kinematic relationship between these two points, P_2 and P_3 , is:

$$A_2 = A_3 \Rightarrow A_2/3$$

or since both points lie on the same rigid body

$$A_{211} \leftrightarrow A_{212} = A_{311} \leftrightarrow A_{312} \leftrightarrow (d_{2/3}) \propto \leftrightarrow (d_{2/3}) \omega^2$$
 (7)

where: d2/3 = Relative distance between P_2 and P_3

Since the first four quantities (from left to right) are known in both direction and magnitude from the accelerometer outputs and the distance between the points is also known, as well as the directions of the relative acceleration terms, this vector equation can be solved for the two unknown magnitudes, α and ω .

Knowing α and ω , a relative acceleration equation can be written between either P_2 or P_3 and the c.g., P_1 . This equation is

$$A_1 = A_2 \Rightarrow A_{1/2}$$

or in component form

$$A_{111} + A_{112} = A_{211} + A_{212} + (d_{1/2}) \propto + (d_{1/2}) \omega^2$$
 (8)

Since the distance between P_1 and P_2 (d_{12}) can be measured, all the quantities on the right-hand side of the equation are known in both direction and magnitude. Consequently, this vector equation can be solved for the desired components of the acceleration of the c.g., A_{111} and A_{112} .

With these accelerations determined, Eqs. 4-6 can be used to obtain the neck reactions.

Subjects — Two different types of anthropomorphic dummies, two cadavers, and a human volunteer were used as subjects for the simulations. The geometric and inertial properties of the Alderson Model F5-AU and the Sierra 50th percentile, vertebrae dummies are listed in Table 4, and their relative joint stiffnesses are presented in Table 5.

The neck of the Alderson dummy, which consisted of three steel segments, was modified by the insertion of thin pieces of rubber between each of the neck segments. These rubber interfaces attenuate the high frequency acceleration which occurs when two adjacent neck segments "bottom out." The head and neck segments were fastened to the torso by means of a steel cable. The tension in the cable was used to regulate the stiffness of the neck. Relative rotation of the head with respect to the torso in the sagittal plane was approximately ± 65 deg.

The neck assembly for the Sierra dummy consisted of seven steel segments, ball and socketed together. The ends of the assembly were bolted rigidly in place to the head and torso, respectively. The relative stiffness between adjacent segments is individually adjustable. A sandwich-type rubber disc consisting of a thick layer of spongy rubber between two layers of thin, hard rubber between each pair of segments prevented metal-to-metal contact between vertebrae. The allowable sagittal rotation of the head with respect to the torso without these interfaces was ± 72 deg, and was somewhat less with them in place.

Table 6 lists the pertinent information for the two cadavers and volunteer. Dummy 1 had the heaviest head, 12.1 lb, as compared to 11.4, 6.3, 9.1, and 10.8 lb for dummy 2, cadavers 1035 and 1089 and the volunteer, respectively, but was classified by the manufacturer as a 5th percentile dummy.

Instrumentation — A complete listing of the types of transducers used and the corresponding conditioning and read-out systems are presented in Table 7. The sled

Table 4 — Geometric and Inertial Properties of Dummies

	Length,		C.G. Position,		Weight, Ib		CG, 2	
Dummy Segment	1º"	2 ^b	1 2		1 2		1 2	
Head - c.g. measured from head pivot; length to top of head	6.1	7.3	1.1	2.2	12.1	11.4	0.29	0.31
Neck - c.g. measured from torso pivot point; length to head pivot	5.5	5.5	2.3	2.5	2.5	4.4	0.04	0.03
Torso - c.g. measured from H-point; length to pivot point of 1st neck vertebra	19.9	21.5	9.5	11.8	35.5	66.0	3.29	8.31
Upper Arm ^C - c.g. measured from shoulder pivot; length to elbow pivot	10.6	11.4	2.9	5.1	7.7	4.5	0.35	0.17
Lower Arm and Hand - c.g. meas- ured from elbow pivot; length to fingertips	17.1	17.5	6.6	7.4	4.0	4.6	0.24	0.26
Upper Leg - c.g. measured from H-point; length to knee point	16.4	16.9	6.4	7.3	14.4	16.5	1.26	1.37
ower Leg, Foot and Shoe - c.g. measured from knee pivot; length to sole of shoe	19.9	20.6	13.4	11.3	12.0	11.6	1.60	1.54

^a Dummy 1 - Alderson F5-AU, 5th percentile, vertebraed with rib cage, weight 124 lb, height 66 in.

NOTES: Weights and moments of inertia of arms and legs for right side only.

Methods of measurement similar to those described by Naab (5).

^bDummy 2 - Sierra No. 292-750, 50th percentile, vertebraed with rib cage, weight 159 lb, height 71 in.

^CUpper arm for dummy 2 does not include shoulder pivot shaft.

instrumentation consisted of a sled accelerometer and a velocity transducer. Seat back resisting torque and rotation were monitored when the back was allowed to rotate. When used, the sagittal headrest load was measured by two axes of a triaxial load cell.

All subjects' heads were instrumented at two points with two uniaxial accelerometers whose axes were orthogonal. In the case of the dummies the accelerometers were mounted within the head cavity, a pair posteriorly mounted and a pair anteriorly mounted. For the cadavers one pair of accelerometers was screwed to the superior portion of the skull and the other pair was mounted to dental acrylic which was molded to the interior of the oral cavity and protruded through the mouth. For the volunteer a pair of accelerometers was mounted to a fitted biteplate made of dental

Table 5 -	Relative	Joint Stiffnesses	of Dummies

Joint	Loc	•	Momei f	nt Arm, t	Moment, ft-Ib		
	1 a	2 b	1	2	11	2	
Head	12.9	6.5	0.23	0.33	3.0	2.2	
Hip	6.3	7.5	2.00	1.00	12.6	7.5	
Knee	34.5	2.5	1.00	1.00	34.5	2.5	
Shoulder	22.5	2.3	1.00	1.00	22.5	2.3	
Elbow	23.0	9.0	0.78	1.00	17.9	9.0	

^a Dummy 1, Alderson, see Table 4.

NOTES: Inferior end of moment arm for head taken as pivot point of head with respect to neck, P 8. Values for dua! segments are averages of right and left sides.

Table 6 - Cadaver and Volunteer Statistics

						Head Po	rameter	s		
Subject	Age, Wt., Ht., Wt., yr Ib in. Ib		I _{CG, 2} Circum., Width, lb-insec in. in.			Length (A-P), in.	Hip to Shoulder, in.			
Cadaver 1035ª	66	134	64	6.3	.11	20.8	5.7	7.4	1.8	21.5
Cadaver 1089 ^b	69	130	67	9.1	.19	24.0	6.5	7.9	2.4	23.5
Volunteer (LMP)	47	160	68	10.8	.20	22.3	5.9	7.5	2.4	21.5

NOTES: Head parameters for cadavers taken from their decapitated heads.

All subjects were male.

^b Dummy 2, Sierra, see Table 4.

Head parameters for volunteer estimated from cadaver data using method described in Ref. 6 and the Ph.D. dissertation, "Kinematics and Kinetics of Whiplash," by H.J. Mertz, Jr., Wayne State University. 1967.

Table 7 – Transducer, Electronic Conditioning, and Recording Details

Trace	Transducer	Amplification	Galvanometer Frequency ^a	
Head acceleration	Statham accelerometers, Models A52-100-350 and A6-100-350	Heiland carrier amplifier, Model 119-B1	1650	
Head load cell	2 axes of triaxial strain gage load cell (G.M. and W.S.U. design)	Heiland carrier amplifier, Model 119-81	1650	
Seat back torque	Strain gaged seat shaft	Heiland carrier amplifier, Model 119-81	3300	
Seat back rotation	Rotary potentiometer used in Wheatstone bridge	Kin Tel amplifier, Model 112A	Tape ^b	
Lap belt load	Strain gaged axial load cells	Heiland carrier amplifier, Model 119-B1	Tapeb	
Sled acceleration	Statham accelerometer, Model A5-100-350	Kin Tel amplifier ^c , Model 112A	1650 ^d and tape	
Sled velocity	Magnetic pickup	None	5000	

^a Data recorded using either a Honeywell Visicorder Model 906A with Honeywell subminiature galvanometers and/or an Electro-Medi-Dyne 8 channel 1/2 in. tape recorder (linear to 5000 cps at tape speed of 15 ips).

b Trace recorded using M1650 galvanometer when head load was not measured.

d Output recorded with both galvanometer and tape for synchronization.



Fig. 5 — Head instrumentation of volunteer

^c For runs when cadaver 1089 was used, no amplification needed because a very sensitive M100-120 galvanometer was used to filter high frequency structural vibrations. Bridge output shunted by 175 ohm resistor to critically damp this galvanometer.

acrylic (Fig. 5). The other pair was attached to a plastic headband in the forehead region. Axial load cells were used to measure the seat belt loads.

Because of the multiplicity of transducer channels, two different read-out systems, tape and oscillograph, were employed. Synchronization between these systems was accomplished by splitting the sled acceleration trace and timing signal and recording both on each system.

High-speed cinematography of all simulations was obtained using a 16 mm, 500 f/sec, 160 deg shutter Milliken camera Model No. DSM-4B with a Kodak Cine Ekta 25 mm, f1.4 lens. The camera was placed 18 ft from the vertical plane containing the sagittal plane of the subject. The film used was Ektachrome ERB, high-speed, ASA 125. Film speed was obtained from a neon bulb flashing every 1/120 sec. Synchronization between the film and the transducer outputs was obtained by firing a flash bulb at sled contact with the snubber and recording the firing voltage with a galvanometer.

Procedure - For both dummies and both cadavers the simulation sequences were with minor exceptions identical. Two series, one with the head supported followed by one with no head support, were conducted using these subjects. For the head supported series, the first run was with a rigid seat back at the nonsevere, 9 mph and 10 in. stopping distance condition. The remaining runs of the series were conducted at the severe level, 15 mph and 17.5 in. stopping distance. The degree of seat back rigidity was incrementally increased with the seat back being rigid for the last run of the series. The simulation sequence for the case of no head support was identical.

Similarly, the simulation sequence for the volunteer consisted of two series, head supported and unsupported. However, for the supported head series the first run was conducted at 9 mph and 22 in. stopping distance with the severity of each succeeding run being increased. The most severe run was 14.7 mph with a 10 in. stopping distance. After this run the volunteer was still willing to undergo higher severity runs, but because of fatigue further runs at increased severity were not conducted. Two runs were conducted with no head support, the first at 8.4 mph and 22 in. stopping distance and the second at 8.9 mph and 10 in. stopping distance, which correspond to the non-severe simulation condition. After the last run the volunteer expressed the opinion that he did not care to increase the severity level at that time. In all cases for the volunteer the seat back was rigid.

Three different restraint systems, free, lap belted, and lap and diagonal chest belted, were employed with the Alderson dummy. However, preliminary runs indicated that no load was applied to the chest straps. Consequently, all other subjects were restrained only by a lap belt. The headrest used for the Alderson dummy was curved, for the Sierra dummy the curved surface and a flat surface were employed, and for the cadavers and volunteer only the flat surface headrest was used.

When cadavers were used as subjects, a preliminary set of X-rays of the cervical spine was taken before they were subjected to the simulation. Subsequent sets of X-rays were taken after any simulation in which damage to the cervical spine was suspected to have occurred. All X-ray sets consisted of three lateral shots of the cervical spine with the neck in normal, flexed, and extended positions; an anterior to posterior shot of the head, neck, and upper thoracic vertebrae with the head in a normal position; and a posterior to anterior shot of the cervical spine with the head extended so as to reveal the odontoid process.

Method of Data Analysis - All the traces on the oscillograph records of each simulation were read out in various time increments. From the high-speed film the frames corresponding to these time increments were analyzed for relative head position and seat back angle. These data were used as input information for a computer program which calculated, based on Eqs. 4-8, the acceleration of the c.g. of the head, the angular acceleration and velocity of the head, and the corresponding neck reactions for each time increment. Also, the computer program corrected each pair of accelerometer readings to give the acceleration at points described by the intersection of their sensitive axes.

Results and Discussion

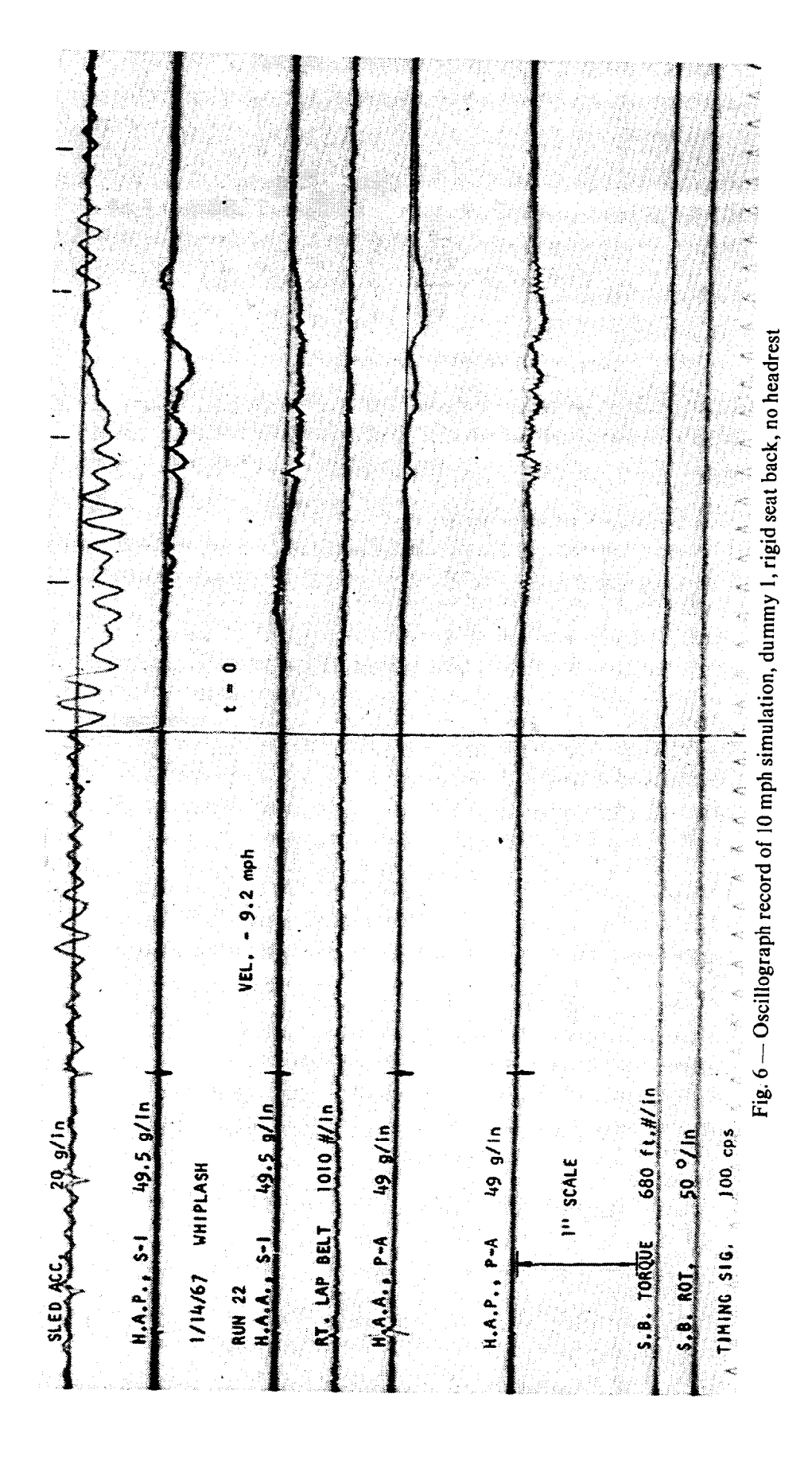
Comparison of the Responses of Various Subjects With No Headrest - The first comparison is for the case where the subjects, with the exception of the volunteer, who underwent only the 10 mph simulation, were subjected to the simulated 10 and 23 mph rear-end collisions without a headrest. In each simulation the subject was lap belted, and the seat back was not allowed to rotate.

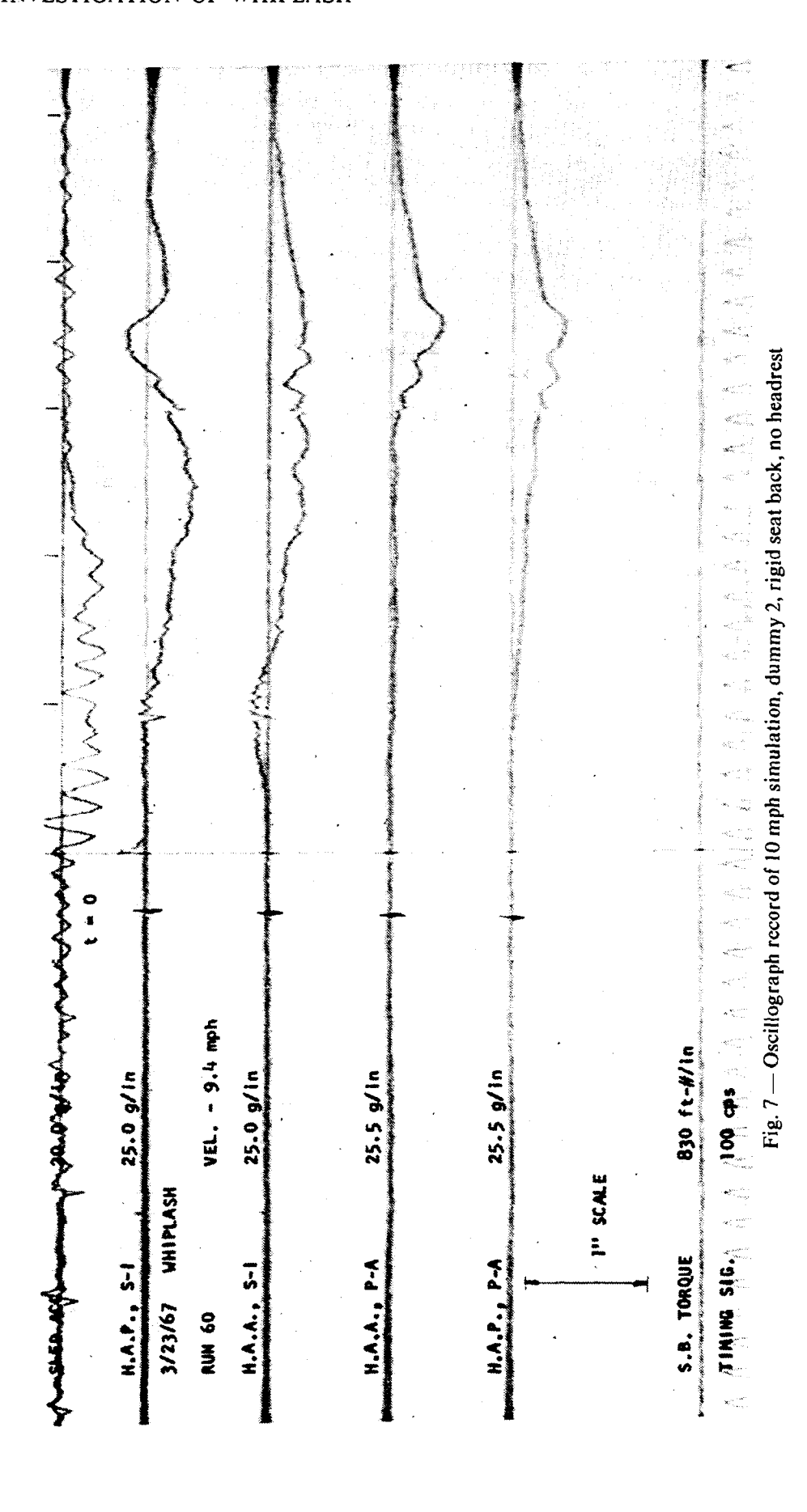
The oscillograph records for the various subjects are presented in Figs. 6-14. The head acceleration traces are identified by three letters. The first two letters, H.A., signify head acceleration, while the third letter designates the anatomical position of the accelerometers as described previously. The symbols S-I (superior toward inferior) and P-A (posterior toward anterior) indicate the approximate direction of the sensitive axis of the accelerometers relative to the head and are indicated by arrows. The vertical line labeled t=0 represents the beginning of the simulated pulse. The small vertical hash marks above the sled acceleration trace subdivide the time after t=0 into 50 ms intervals. The timing signal gives a continuous 10 ms time base. Calibration factors for each trace along with an equivalent 1 in. scale are given.

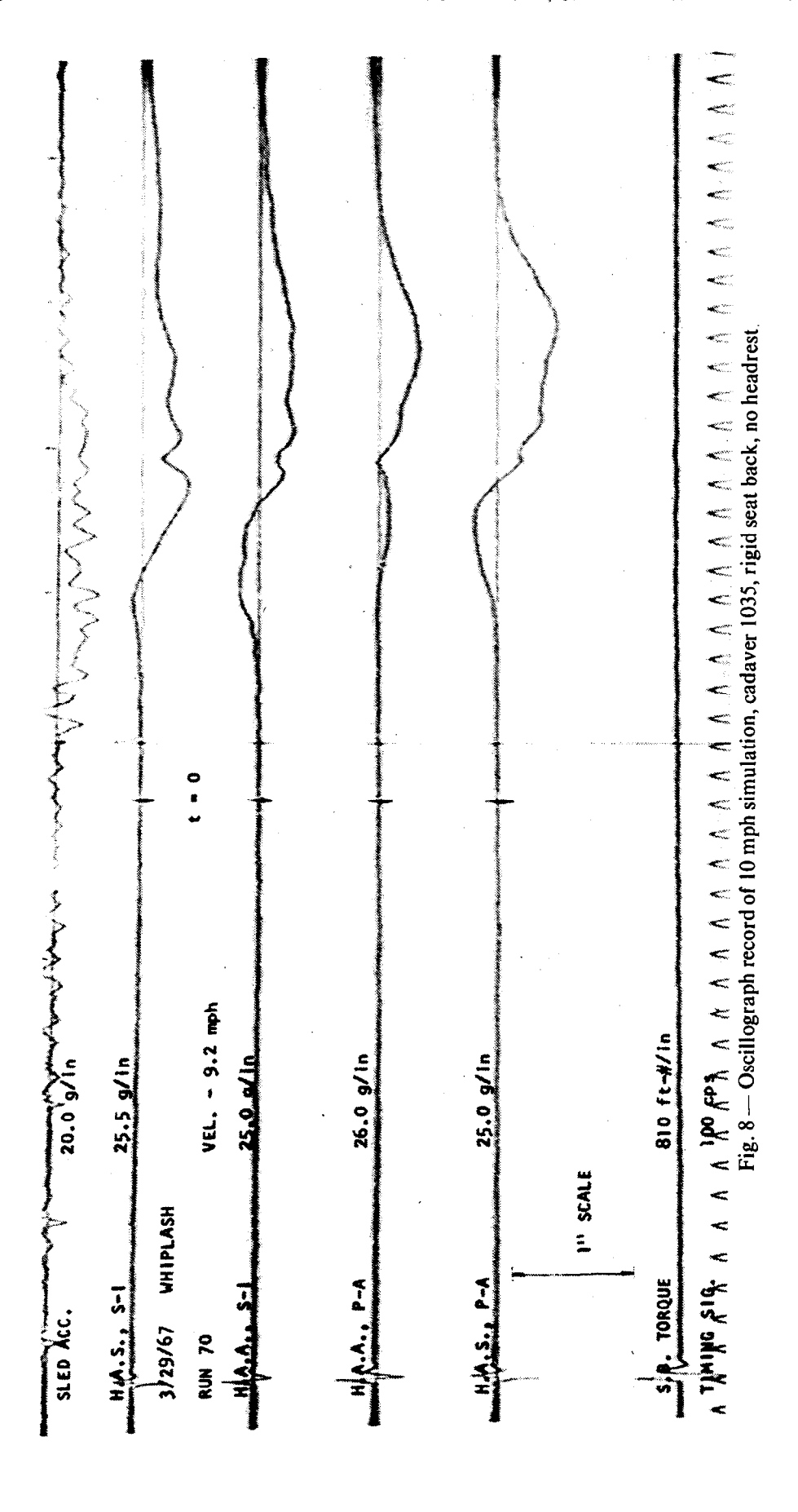
Because of the differences in location of accelerometers of each subject, direct comparison of traces can be made only in special cases and then only when differences in calibration factors are noted. Direct comparison of all traces between dummy 1 with dummy 2 and cadaver 1035 with cadaver 1089 can be made, but comparisons between the traces of the dummies, cadavers, and volunteer can be made only for the anteriorly located accelerometers in the P-A and S-I directions.

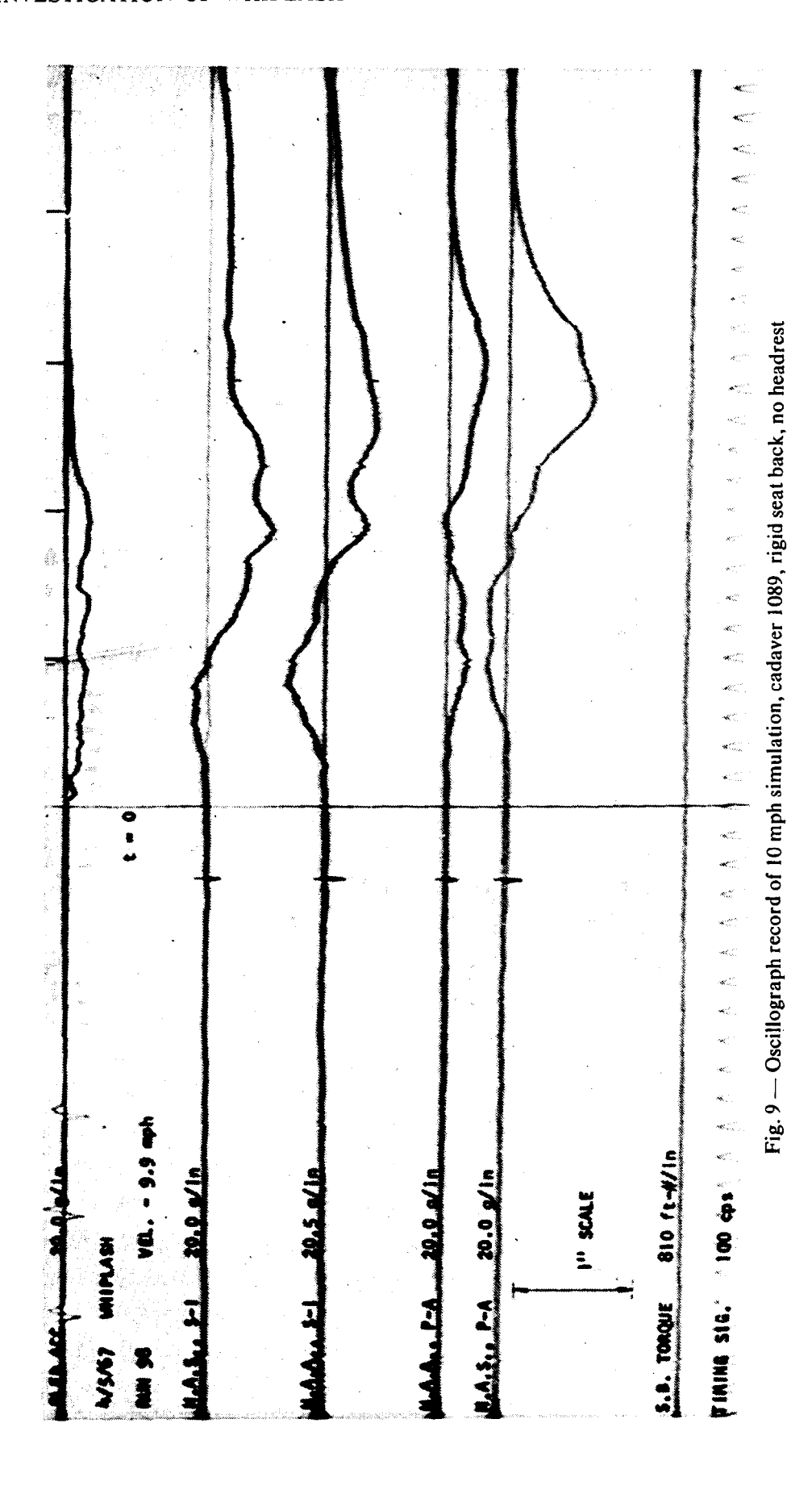
For the 10 mph simulation, the general shapes of the corresponding traces for the two cadavers (Figs. 8 and 9) are in good agreement with each other. The similarity between accelerometer response for the dummies (Figs. 6 and 7) is not good. In particular, the corresponding H.A.P., S-I and the H.A.A., P-A traces are not similar even though the accelerometers are located in identical head positions. The H.A.A., S-I traces for both cadavers and both dummies compare in general shape to the H.A.M., S-I trace (Fig. 10) of the volunteer. The pulse times for the volunteer traces are longer than for the cadavers or dummies due to the tensing of muscles prior to the simulation.

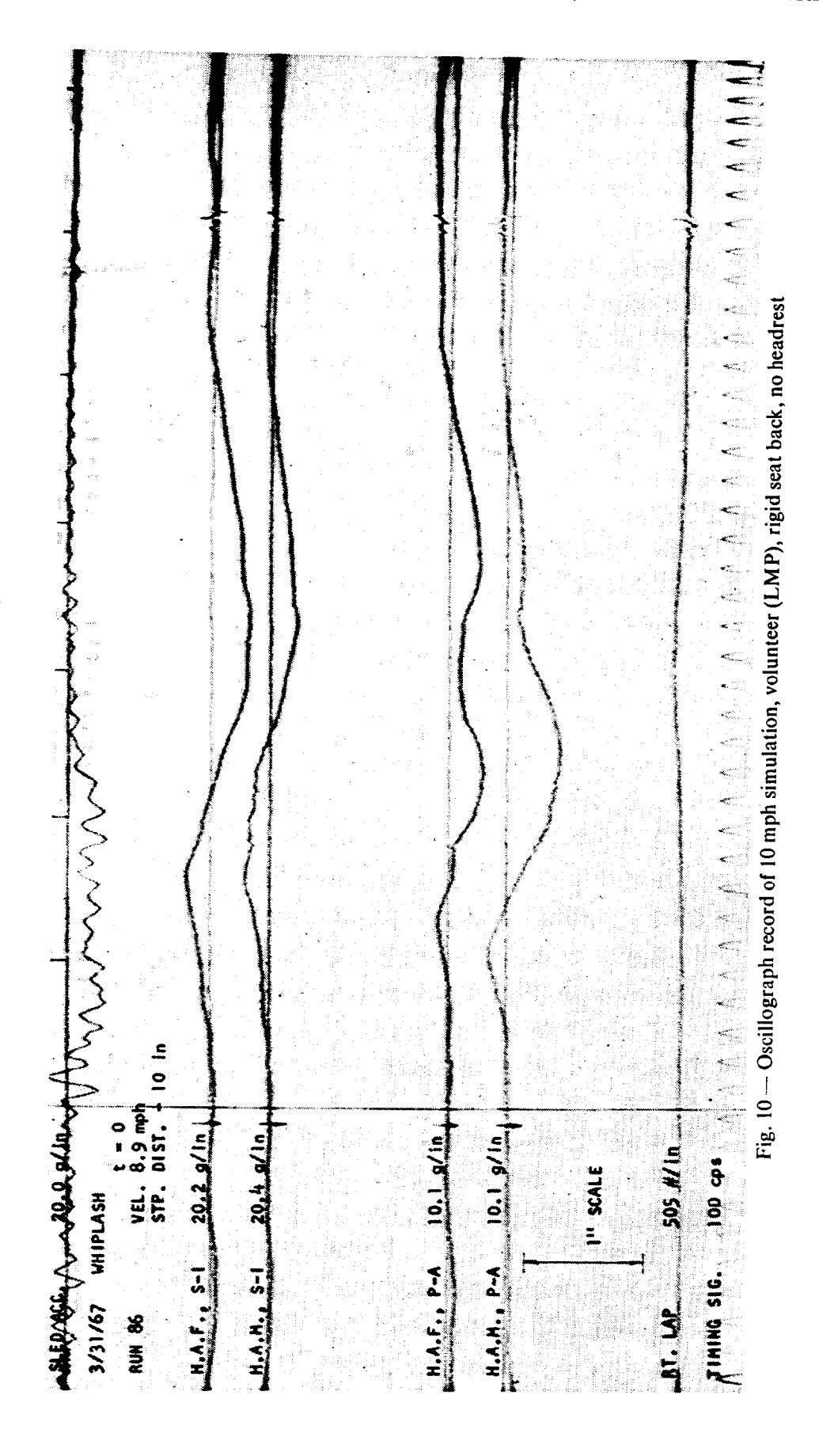
For the 23 mph equivalent rear-end collision, the corresponding traces (Figs. 13 and 14) between cadavers are again in good agreement, while the dummy traces (Figs. 11 and 12) are not. A typical high g artifact caused by metal-to-metal contact of the neck segments is shown on the H.A.A., P-A for dummy 1 at approximately 165 ms (Fig. 11). A similar artifact occurs on all head traces for dummy 2 at approximately

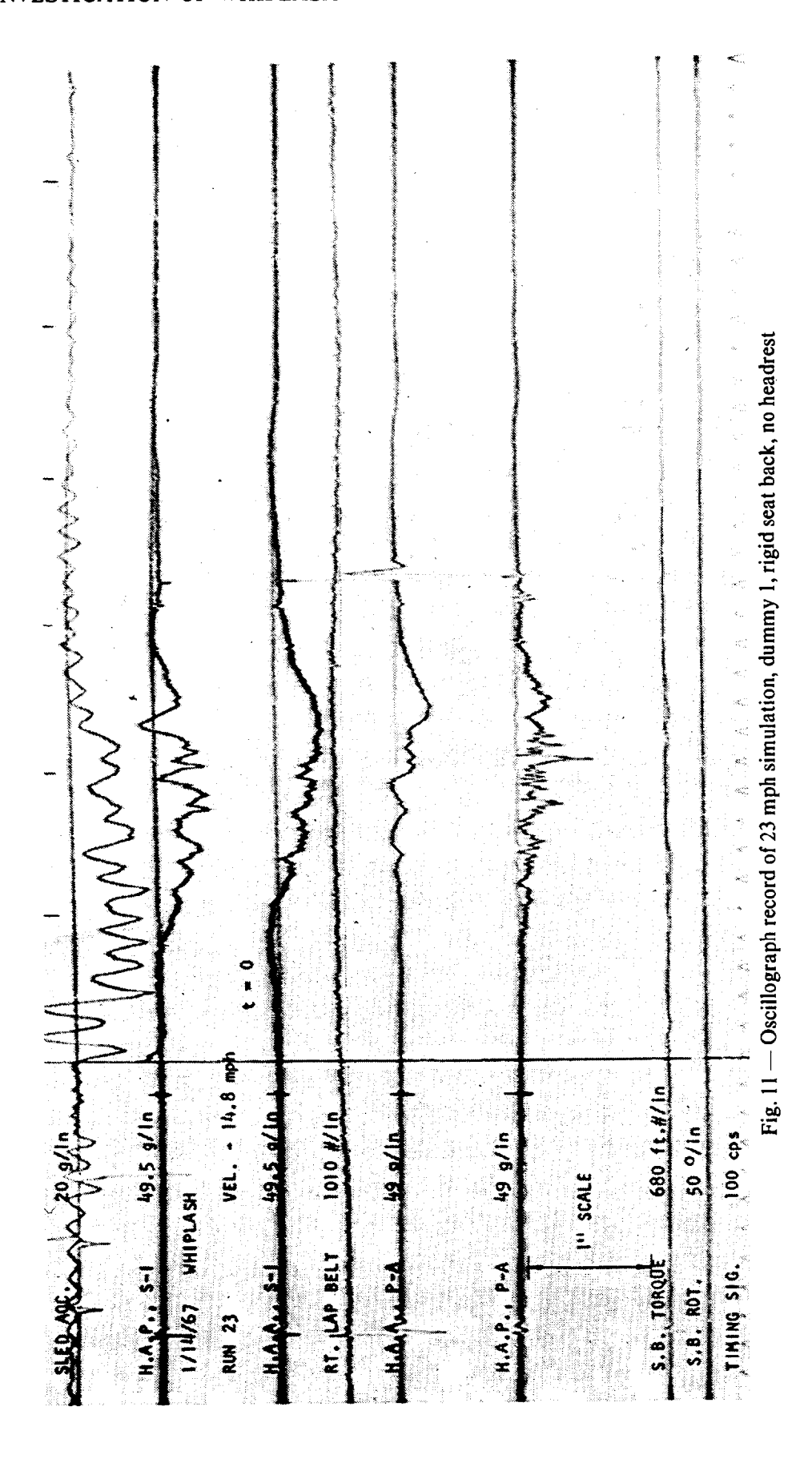


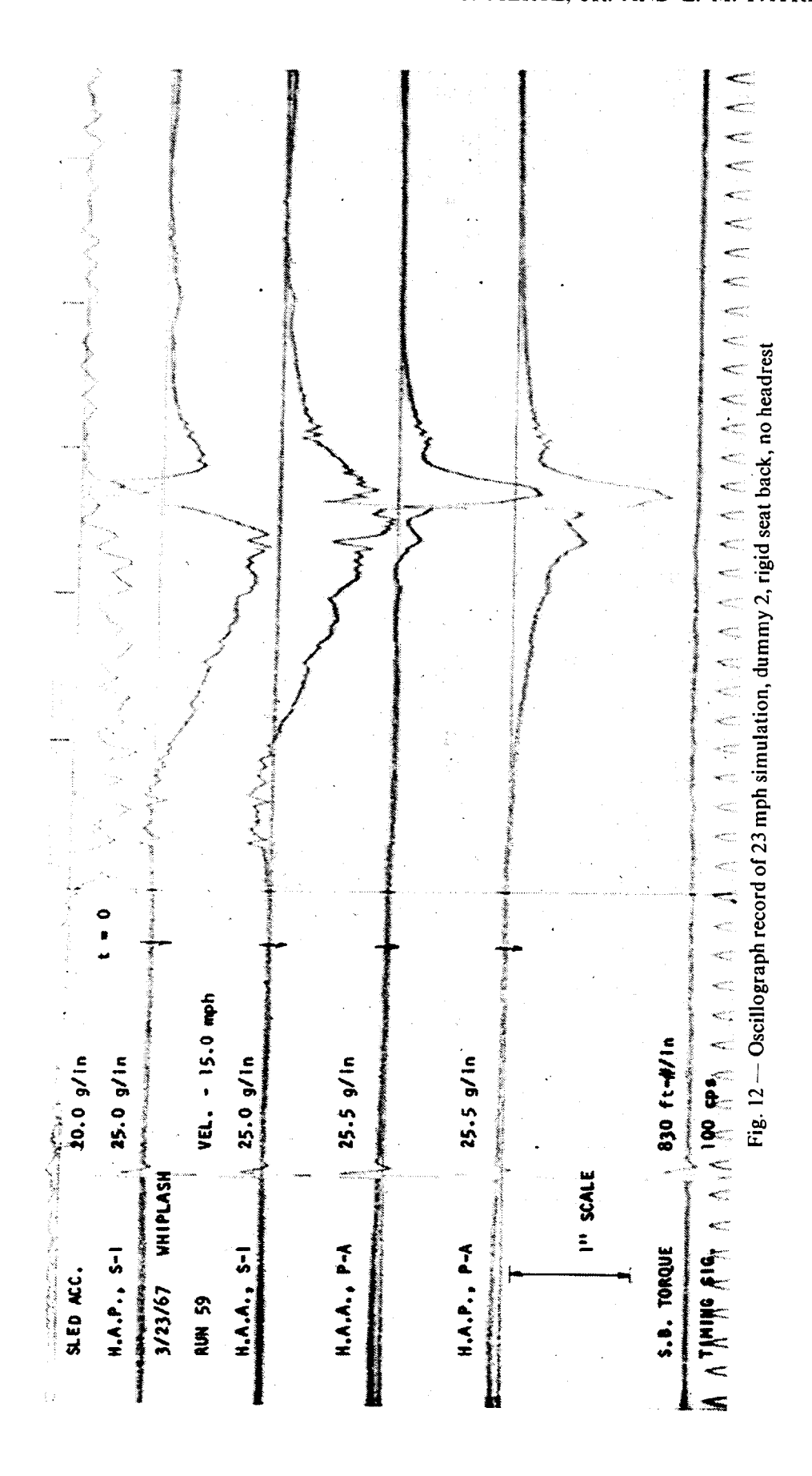


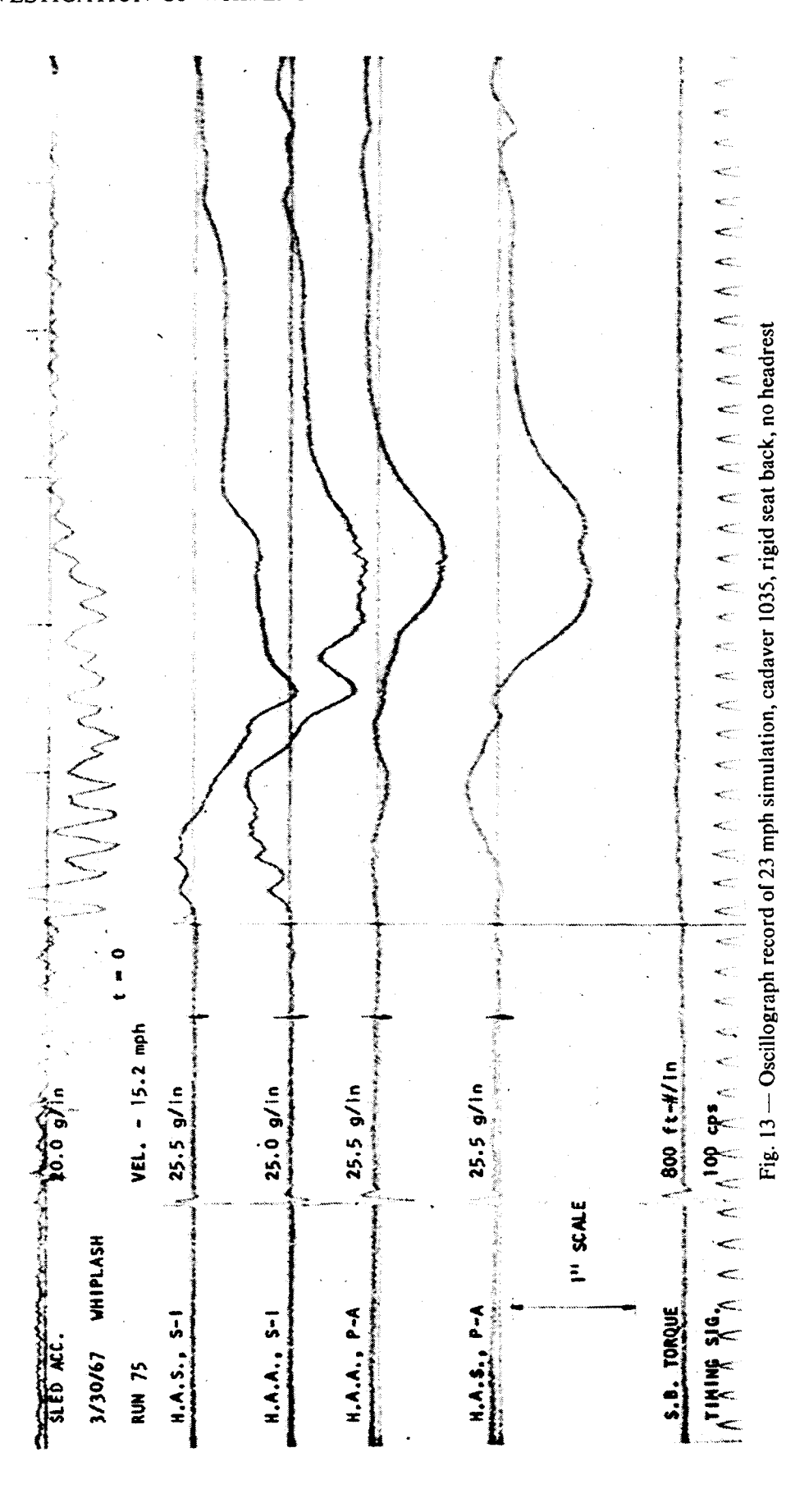


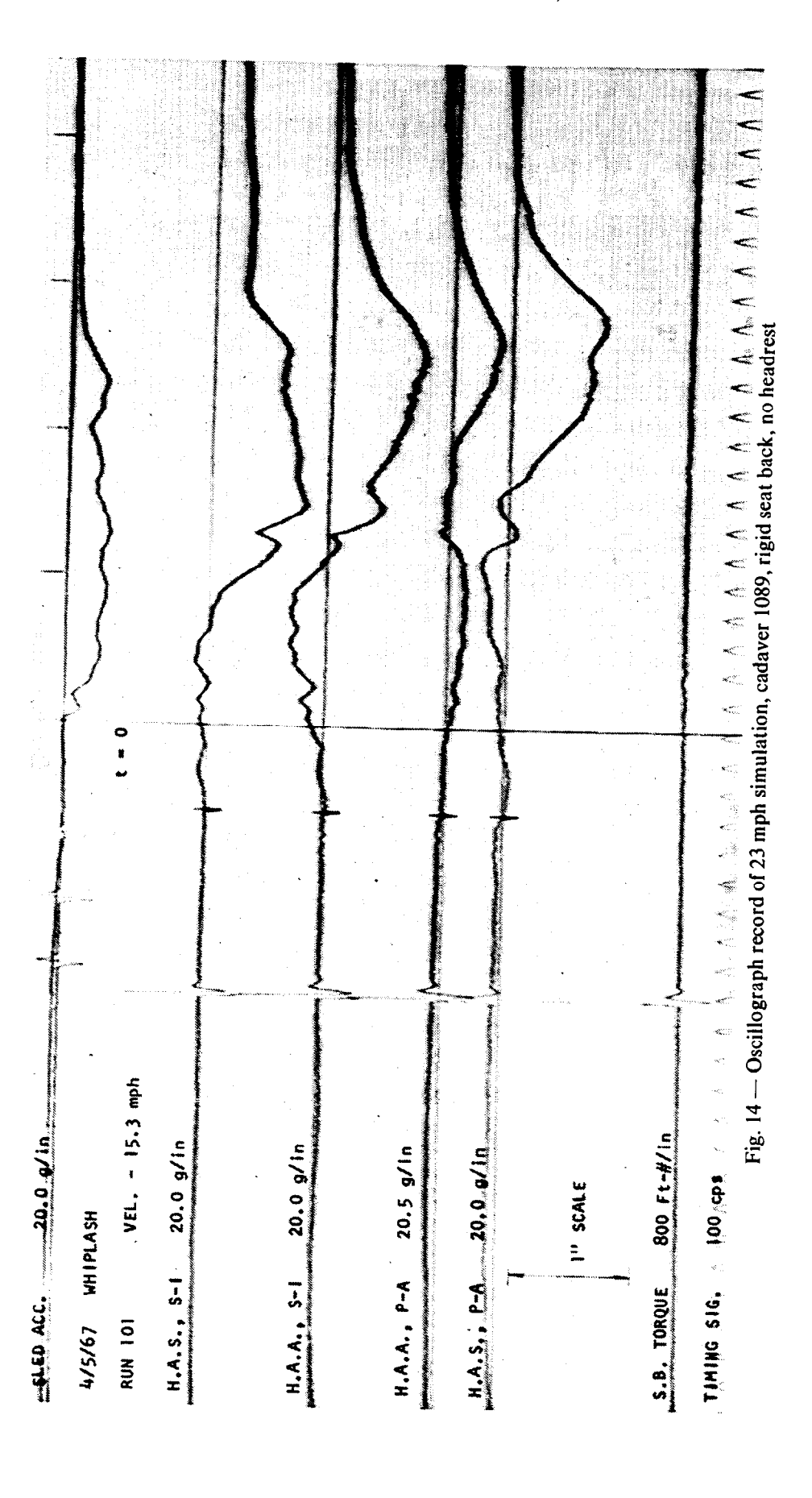












130 ms (Fig. 12). Pieces of rubber were inserted between the segments of the neck of each dummy to attenuate this effect; however, complete elimination would make head instrumentation and record read-out more reliable. Another undesirable trait related to dummy construction is the high frequency oscillation due to local vibration at the accelerometer mount which makes the determination of the rigid body acceleration difficult. None of these artifacts occurred on any of the volunteer or cadaver traces.

An artifact common to all traces for all subjects occurs prior to t = 0 and is the result of a switching transient caused by closing the braking valve for the power cylinder.

Also, depicted on the oscillograph records are two different sled acceleration wave shapes. For simulations involving dummies 1 and 2, the volunteer and cadaver 1035 (Figs. 6-8 and 10-13), the sled accelerometer was wrapped in sponge rubber and enclosed in a box which was mounted to the sled. This eliminated the very high g, short time duration structural vibrations of the sled. The sponge rubber caused a lower g, longer time duration vibration to be superimposed on the rigid body acceleration of the sled. The resulting wave shape was satisfactory since a mean sled acceleration could be approximated. For the sequence of simulations using cadaver 1089 (Figs. 9 and 14), the accelerometer was mounted directly to the sled frame. The output of the accelerometer was not amplified but was fed directly to a sensitive, low frequency, critically damped galvanometer which mechanically filtered the high frequency structural vibrations.

From these oscillograph records the neck reactions, the acceleration of the c.g. of the head, and the head angular acceleration were computed for various time increments using Eqs. 4-8. The computed neck torques acting on the head at the occipital condyles as a function of time for both the 10 and 23 mph simulations for the various subjects are shown in Fig. 15. The dummy's resistive neck torques for both simulation conditions are characterized by high rates of loading, with the response of dummy 2 being more pronounced than that of dummy 1. Considering the neck construction of the dummies, this type of response should be expected. The neck of dummy 1 consists of steel cable. Consequently, the torque needed to produce a change in curvature of the neck depends on the contact surface between segments and the tension in the cable. However, both these quantities vary with neck curvature, resulting in a fluctuation in required torque levels. When relative movement of neck segments is prohibited by metal-to-metal contact (the segments are all bottomed out), further extension of the head takes place primarily by stretching of the steel cable and changing the curvature of the dummy's torso, which requires a large torque increment per degree of rotation. The neck of dummy 2 is constructed of steel segments which are "ball and socketed" together. The torque required to produce a change in curvature of the segments depends upon the rotational frictional resistance of the ball with respect to the socket, which depends on the mating of relative surfaces. Consequently, the torque necessary to produce a change in curvature of the neck fluctuates until all the segments "bottom out." When this occurs, further head extension must produce a change in curvature of the dummy's torso which results in a rapid increase in torque per degree of head extension. Thus, for both dummies if the head still has a velocity relative to the torso when all the neck segments have bottomed out, the neck torque must increase rapidly in order to slow down the head relative to the torso. Comparing the two different types of neck construction with the segments

bottomed out, the required torque per degree of extension for dummy 1 will be less than that of dummy 2 because of the increase in neck curvature due to cable extension for dummy 1. This is demonstrated by comparing the maximum resistive neck torque values for dummy 1 and dummy 2, which are 20.3 and 43.3 ft-lb for the 10 mph simulation and 58.5 and 118 ft-lb for the 23 mph simulation, respectively.

Unlike the responses of the dummies, the resistive neck torques for both the cadavers and volunteer build up gradually and form continuous loading curves. In the case of the cadaver, the resistance to head extension is provided by the stretching of the muscles, tissues, and ligaments of the neck. This type of neck loading can be compared to that of a living person who is unexpectedly subjected to a rear-end collision and does not have time for his muscles to react in order to resist the head extension. In this case the head rotates with very little resistive torque until the anterior neck ligaments become stretched and posterior tissue between the spinous process of the neck vertebrae is compressed. At this point resistive forces which are produced are identical in nature, if not in magnitude, to that of the cadavers.

The volunteer represented the case of a person aware of the impending rear-end collision who tensed his neck muscles in anticipation of the impact. In this case the resistive torque is comprised of muscle reaction during the initial portion of the head rotation with the stretching of tissue and ligaments gradually taking up some of the

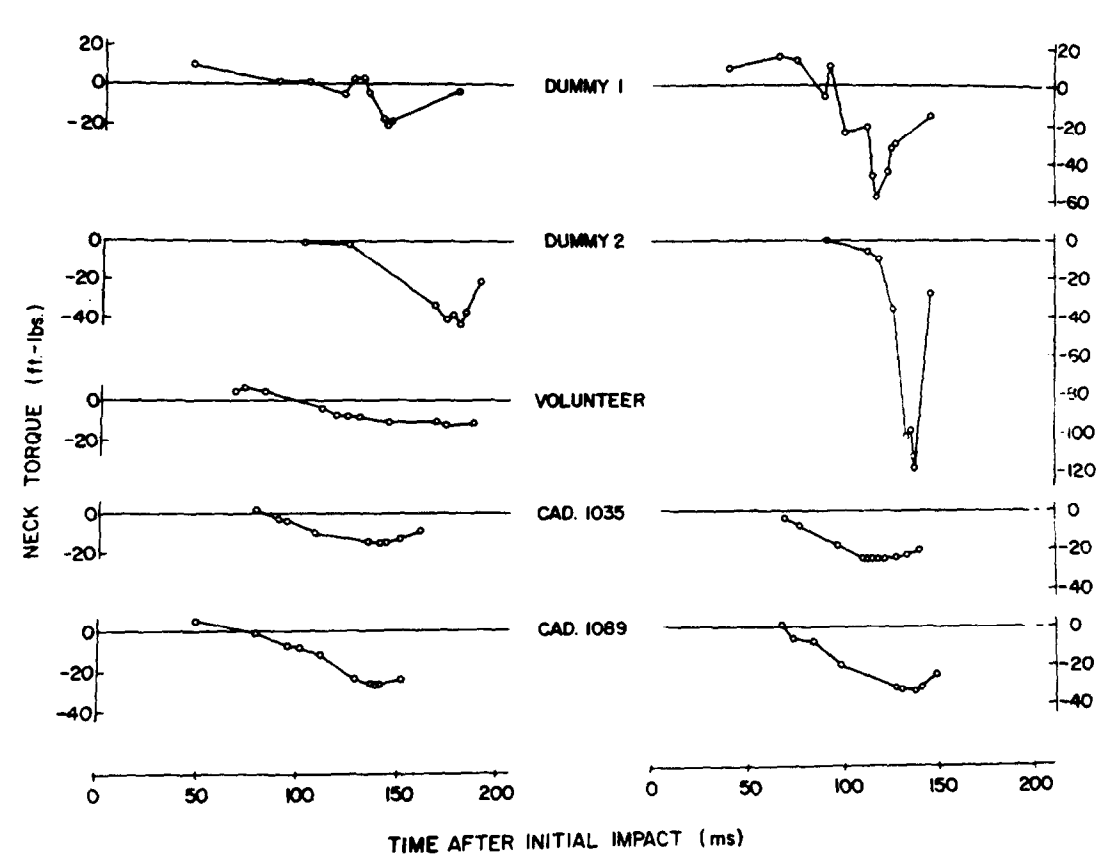


Fig. 15 — Computed neck torques acting on the head at the occipital condyles as function of time for (from left to right) 10 and 23 mph simulations, no headrest, rigid seat back

load as the degree of the extension increases. Since the relative rotation of the head is resisted during the entire head extension for the case of tensing prior to the impact, the maximum neck torque should be less than if the person were not tense. This is verified by comparing the maximum neck torques of 14.9, 27.6, and 12.3 ft-lb for cadavers 1035 and 1089 and the volunteer, respectively, for the 10 mph simulation. Hence, tensing prior to a rear-end collision certainly will reduce the relative severity of the impact.

There was a delay in reaching a peak torque for dummy 2 when compared to the other subjects because the angle through which the head could be rotated prior to bottoming out the neck segments was greater and consequently required a longer time period to reach this position.

The angular acceleration of the head as a function of time for the various subjects for the two simulations is shown in Fig. 16. These curves are similar in shape and relative maximum magnitudes to their corresponding torque curves and portray all the characteristics stated for the torque curves.

The P-A accelerations of the center of gravity of the heads of the various subjects for the 10 and 23 mph simulations are depicted as a function of time in Fig. 17. Again, the smooth, gradually increasing accelerations for the cadavers and volunteer are in contrast to the spiking, variable fluctuating responses of the dummies. The same is

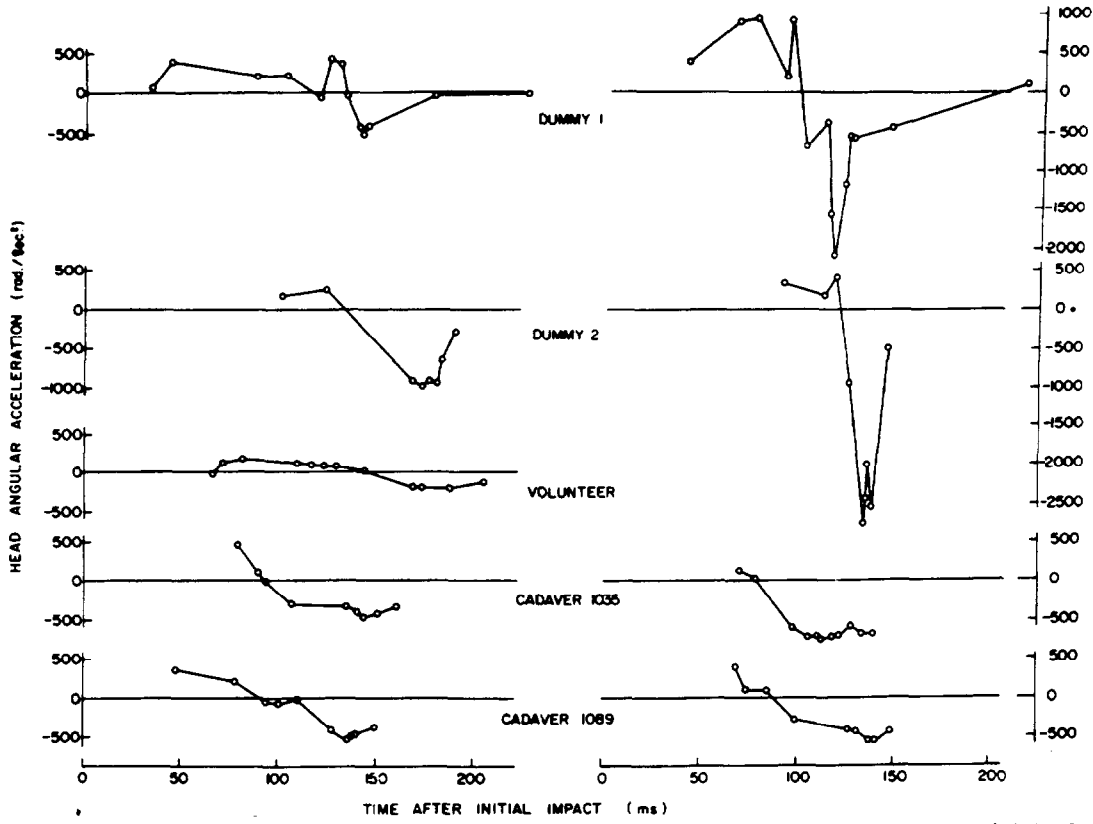


Fig. 16 — Computed head angular accelerations as function of time for (from left to right) 10 and 23 mph simulations, no headrest, rigid seat back

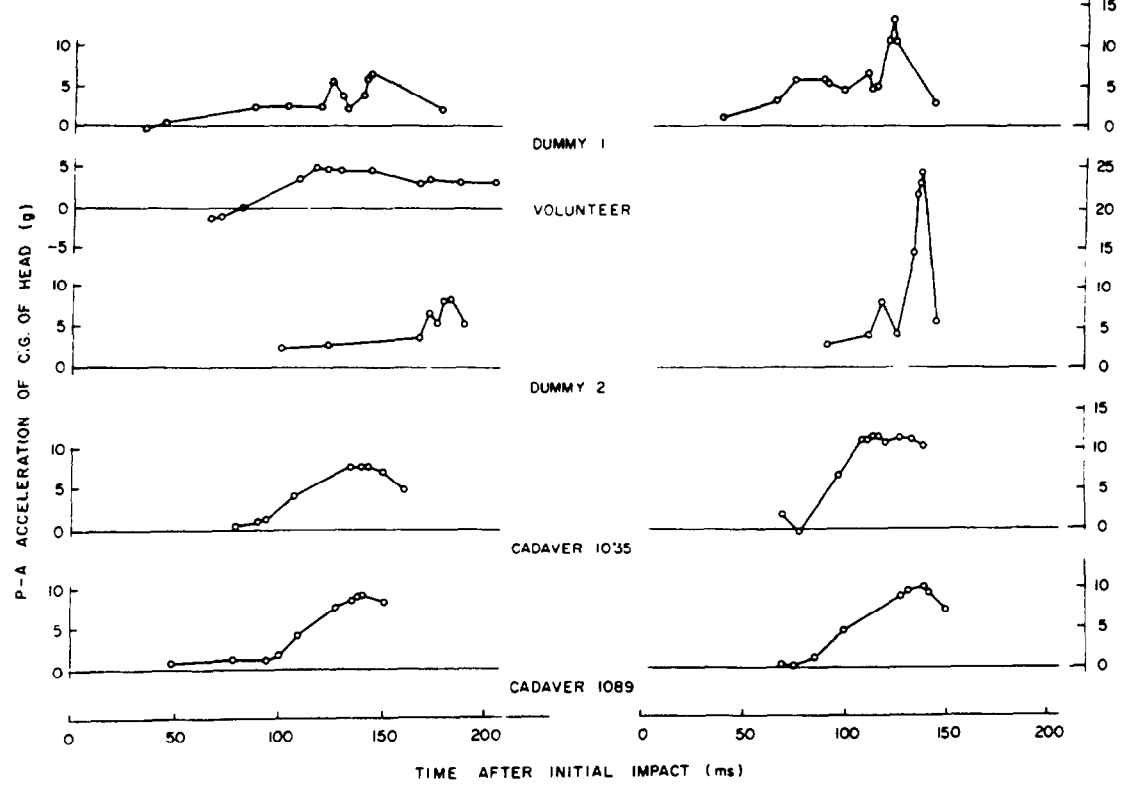


Fig. 17 — Computed P-A acceleration of head c.g. as function of time for (from left to right) 10 and 23 mph simulations, no headrest, rigid seat back

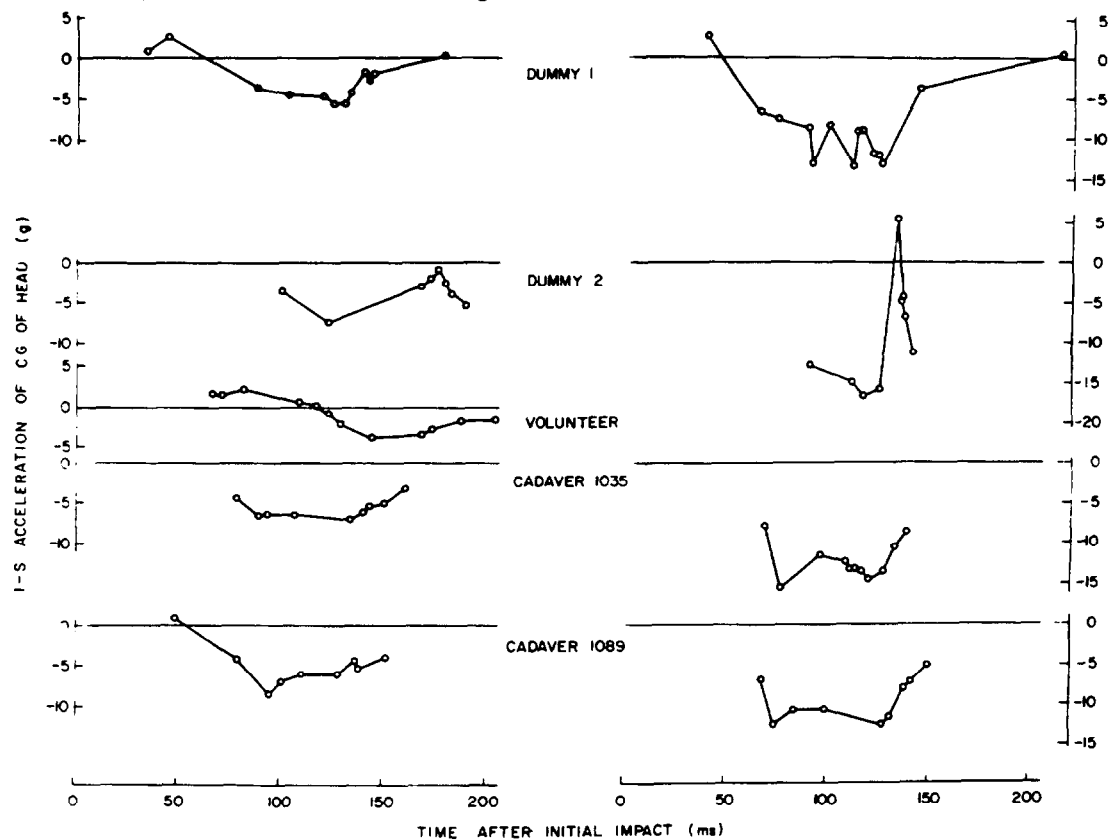


Fig. 18 — Computed I-S accelerations of head c.g. as function of time for (from left to right) 10 and 23 mph simulations, no headrest, rigid seat back

true in general for the I-S curves for the acceleration of the c.g. of the heads of the various subjects presented in Fig. 18.

Comparisons of the relative rotations of the heads of the various subjects for the 10 and 23 mph simulations are presented in Figs. 19A and 19B, respectively. The relative position of the head with respect to the torso was obtained from the film analysis and represents the angular position of the X_{112} (I-S) axis of the head with reference to upper torso. The angle for zero extension of the neck was obtained by measuring the angle between the X_{112} axis of the head and the upper torso with the subject seated in a normal position and was taken as -15 deg for all the subjects.

For the 10 mph, nonsevere simulation the maximum head-neck extensions for dummy 1 and cadavers 1035 and 1089 were in good agreement with each other and were 63, 64, and 61 deg, respectively. The maximum head extension for dummy 2 was 93 deg, 30 deg greater than for dummy 1. For the 23 mph simulation, the maximum head extension for dummy 1 and cadavers 1035 and 1089 were approximately the same—87, 86, and 84 deg, respectively. The maximum head extension of dummy 2 was 104 deg.

The greater head extension for dummy 2 which occurred at both simulation levels was due to the fact that the head-neck combination of dummy 2 allowed a greater relative rotation of the head with respect to the torso prior to bottoming of all the individual neck segments. This greater rotation can be reduced by the removal of one of the neck segments.

Comparing the shapes of the extension curves for the time after the maximum head extension has occurred, the response of dummy 1 is more damped than the response of either cadaver. To decrease this damping effect for dummy 1, the neck segments could be encapsulated in a rubber tube capable of storing energy during the extension motion.

The maximum extension of the volunteer's head and neck for the nonsevere simulation was 27 deg which, because of muscle action, is less than the other subjects. In fact, the volunteer rotated his head forward 10 deg in anticipation of the ensuing extending motion. The shape of the head rotation curve for the volunteer after maximum extension has occurred is similar to the rotation curves for the cadavers, indicating that sufficient energy was stored in the neck during extension to cause the head to rebound.

For the 10 mph simulation (Fig. 19A), the head of cadaver 1035 was extended 17 deg at the initiation of the sled deceleration pulse. Consequently, the angular head velocity was less than it would have been if the head were positioned with no initial extension, resulting in a corresponding lower maximum resistive neck torque.

In Table 8 the maximum dynamic head response for the various subjects for the 10 and 23 mph equivalent rear-end collisions are listed. Also, the static voluntary human tolerance levels for the head in an extended position are presented. The indices listed give a method of comparing the responses of the various subjects to identical simulations based on the static voluntary human tolerance levels, taking into account the differences in head weights. Since the dynamic neck reactions are directly proportional to their corresponding head weights, the effect of the differences in head weights was eliminated by dividing the maximum values of the torque, shear, and axial forces by their corresponding head weights. To compare these ratios with the static voluntary human tolerance levels, the volunteer static levels were divided by the

volunteer's head weight. The indices which allow for direct comparison between subjects were formed by dividing the dynamic ratios by the corresponding static ratio.

An index number of unity or less indicates that the maximum reaction is either equivalent to or less than its corresponding static voluntary tolerance level and no injury is expected. To evaluate the indices which are greater than unity, the response of the cadavers must be considered. Analysis of X-rays indicated that minor ligamentous damage occurred between the third and fourth cervical vertebrae for cadaver 1035, while no damage was observed for cadaver 1089. Since ligamentous damage occurred for a neck torque index of 2.50 and not for an index of 2.25, a

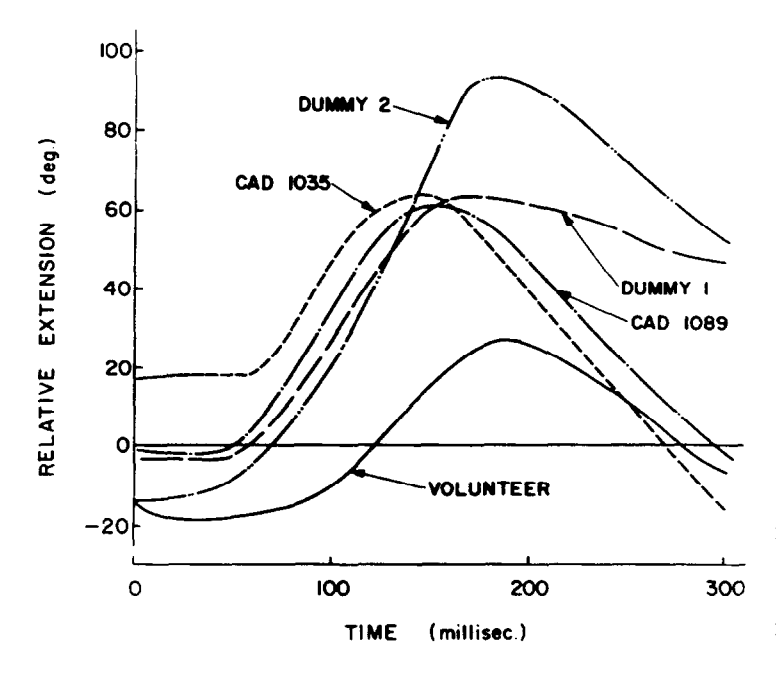


Fig. 19A — Comparison of relative head extension for various subjects for non-severe 10 mph simulation, no headrest, rigid seat back

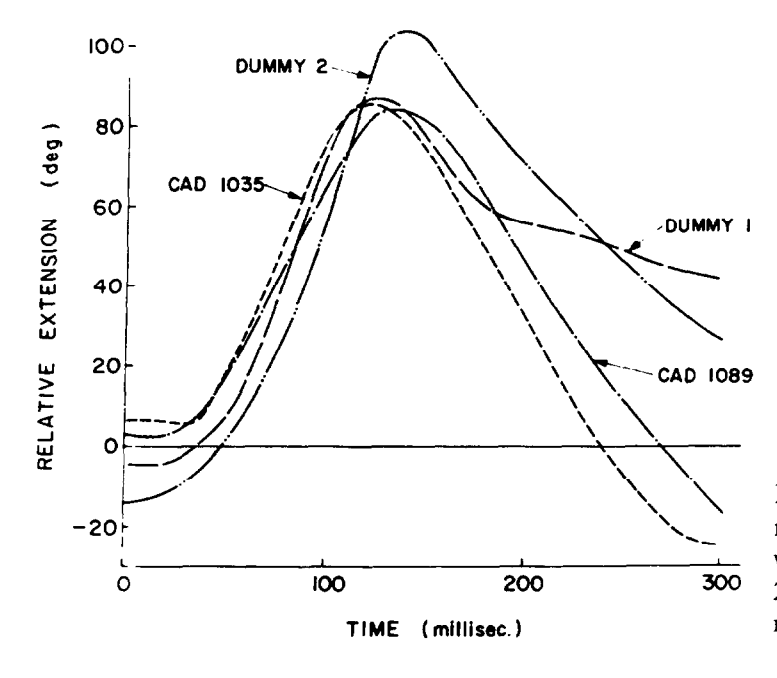


Fig. 19B — Comparison of relative head extension for various subjects for severe 23 mph simulation, no headrest, rigid seat back

tolerable index is less than 2.50 if the cumulative effects of multiple impacts are neglected. Considering the severity of a 23 mph rear-end collision, where the individual with his head in a normal upright position is not aware of the impending impact, neck discomfort and/or injury would be expected and more so in these simulations since the seat back was rigid and corresponds to rear-end collisions of higher velocity. Consequently, the index value of 2.25 for cadaver 1089 should also be considered higher than a desirable limit. However, the 10 mph rear-end collision should be tolerable even in the case of the unsuspecting individual. Assuming that the neck index of 1.85 (10 mph simulation) for cadaver 1089 is not injurious, a tolerable neck index probably lies between 1.85 and 2.25. Until further data are available, a value of 2.00 is suggested.

The shear and axial force indices for the various subjects and the various simulations are all less than unity except for dummy 2. This implies that these reactions do not play a dominant role in causation of neck injury due to hyperextension and that the neck torque is the predominant factor. Hence, the response of the various subjects to the two simulations will be compared on the basis of their corresponding neck torque indices. For the 23 mph simulations, the indices for cadavers 1035 and 1089 and dummy 1 were 2.50, 2.25, and 3.00, respectively, while the index for dummy 2 was 6.40. Certainly, the response of dummy 2 is not comparable to the response of the other three subjects. For the 10 mph simulation the indices for cadavers 1035 and 1089 are 1.45 and 1.85, respectively, and are greater than the index for dummy 1, which is 1.05. The index of 2.35 for dummy 2 is still greater than those of the other subjects. Based on these indices, the neck structure for

Table 8 — Comparison of Maximum Dynamic Head Responses Based on Voluntary Static Human Tolerance Levels

					Rigid S	eat Baci	t		Collar Seat	
				Torque		Shear Force		Axial Force		ne
Subject	Head Weight, Ib	Severity ^a	Max. Tor- que, ft-lb	Index	Max. Shear, Ib	Index	Max. Axial, Ib	Index I3	Min. Torque, ft-lb	Index
Volunteer	10.8	Static NS	17.5 12.3	1.00 0.70	190 49	1.00 0.25	255 28	1.00 0.10	-	_
Dummy 1	12.1	NS S	20.3 58.5		89 172	0.40 0.80	61 159	0.20 0.55	_ 34	_ 1.75
Dummy 2	11.4	NS S	43.3 118.0	2.35 6.40	1 <i>07</i> 287	0.55 1.45	76 189	0.30 0.70	- -	-
Cadaver 1035	6.3	NS S		1.45 2.50	55 61	0.50 0.55	42 94	0.30 0.65	- 17	_ 1.65
Cadaver 1089	9.1	NS S	27.6 33.0	1.85 2.25	90 99	0.55 0.60	70 113	0.35 0.55	- 26	_ 1 <i>.</i> 75

^aNS – Nonsevere 10 mph simulation.

⁵⁻Severe 23 mph simulation.

dummy 2 gives consistently higher simulated response for hyperextension of the neck, while dummy 1 gives a lower index for the 10 mph and a higher index for the 23 mph simulation when compared to indices of the cadavers. The index of the volunteer, which is 0.70, indicates that this simulation produced a neck torque which was below the static volunteer tolerance level. The cadaver indices were more than double the volunteer's index, which implies that tensing for a rear-end collision reduces the severity of the impact.

Effect of Seat Back Rotation on Reducing Severity of a Rear-End Collision without Employing a Headrest - Figure 20 depicts a typical oscillograph record (dummy 1, 23 mph simulation, no headrest) for the case where the seat back was allowed to rotate at a prescribed torque controlled by a frictional torque limiter.

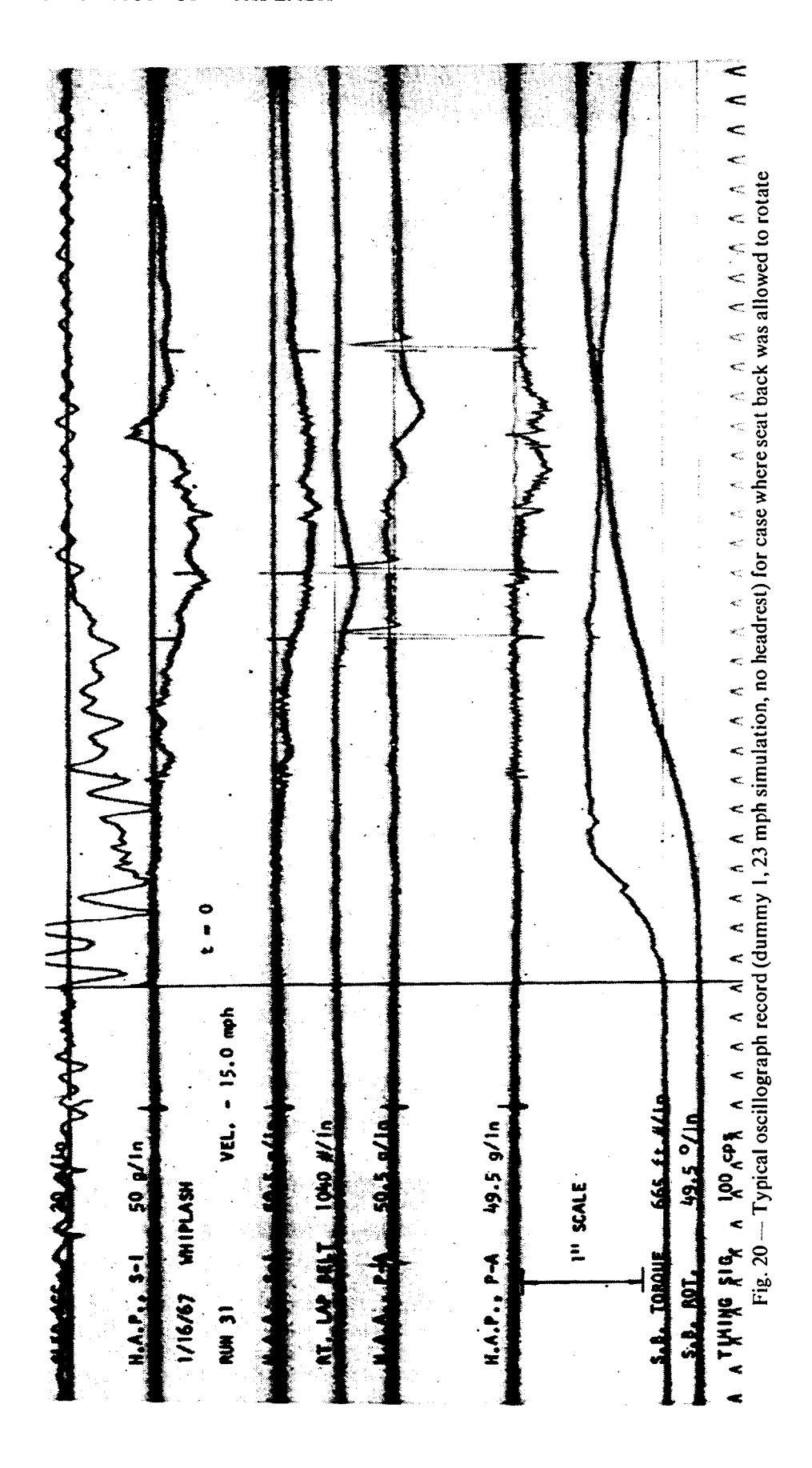
The correlation between the degree of seat back rotation and the resulting maximum resistive head torque for various subjects for the 23 mph simulation is shown in Fig. 21. All the curves demonstrate a decrease in head torque with a decrease in seat back rigidity. The cadavers' curves indicate that an optimum rotational characteristic may exist.

For the comparative cases where the subjects were lap belted, torque indices based on the minimum neck torque for each subject were computed. These indices were 1.75, 1.65, and 1.75 for dummy 1 and cadavers 1035 and 1089, respectively, which when compared to the tolerable index of 2.00 indicate that with sufficient seat back rotation a 23 mph rear-end collision should not be injurious due to hyperextension of the neck. Simulations were conducted with dummy 1 restrained by a lap belt and unrestrained. Without the lap belt restraint, the head torques were lower since the torso moved up the inclined seat back and rotated, resulting in a larger absolute head angle with no increase in the relative angle between the head and the torso. For small changes in seat back angle, the lap belt has little effect on the maximum head torque since there is very little load (60 lb at 20 deg) in the seat belt, as shown in Fig. 22. However, at larger changes in seat back angle the seat belt load is appreciable, 280 lb at 50 deg, tending to increase the resistive head torque by preventing movement of the lower torso.

Comparison of the Responses of the Various Subjects with Headrest - The comparative simulations were again the equivalent 10 and 23 mph rear-end collisions. For each simulation the subject was lap belted in the chair with his head initially in contact with the flat headrest and seat back rigid. The oscillograph records for the 10 mph simulation are shown in Figs. 23-26 for dummy 2, cadavers 1035 and 1089, and the volunteer. Comparison with dummy 1 will not be made since a curved headrest was used and is not directly comparable to the flat headrest used with the other subjects. H. L/C 3-3 designates the head load cell axis normal to the surface, and H. L/C 2-2 designates an orthogonal axis in a vertical plane. The principal load is in the 3-3 direction and will be used to compare subjects. The same restrictions used for the comparison without a headrest on head acceleration traces and relative scale factors still apply. Noting these restrictions, a good comparison between all subjects on the basis of relative wave shape exists. This is also true for the comparable traces on the oscillograph records for the 23 mph simulation shown in Figs. 27-30.

Based on maximum normal headrest load shown in Fig. 31 for the equivalent 10 and 23 mph impacts, the headrest loads of the cadavers and dummy compared quite favorably with those withstood by the volunteer.

Because of the uncertainty of locating the point of application of the headrest load



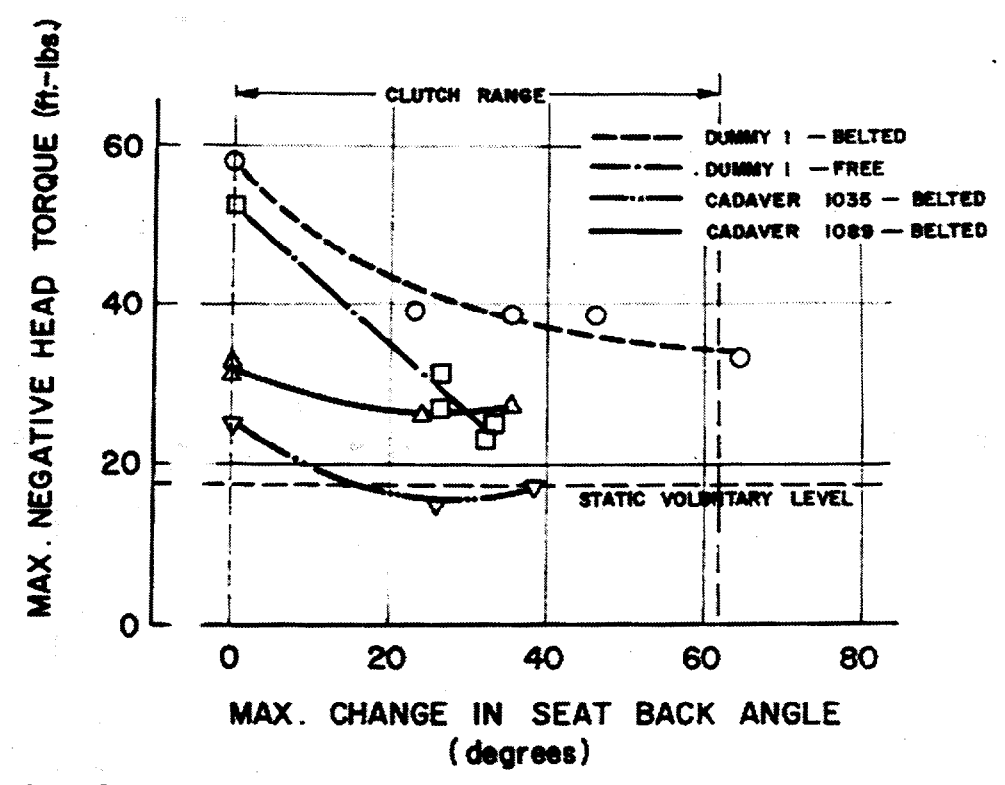


Fig. 21 — Comparison between degree of seat back rotation and resulting maximum negative neck torque for 23 mph simulation, no headrest

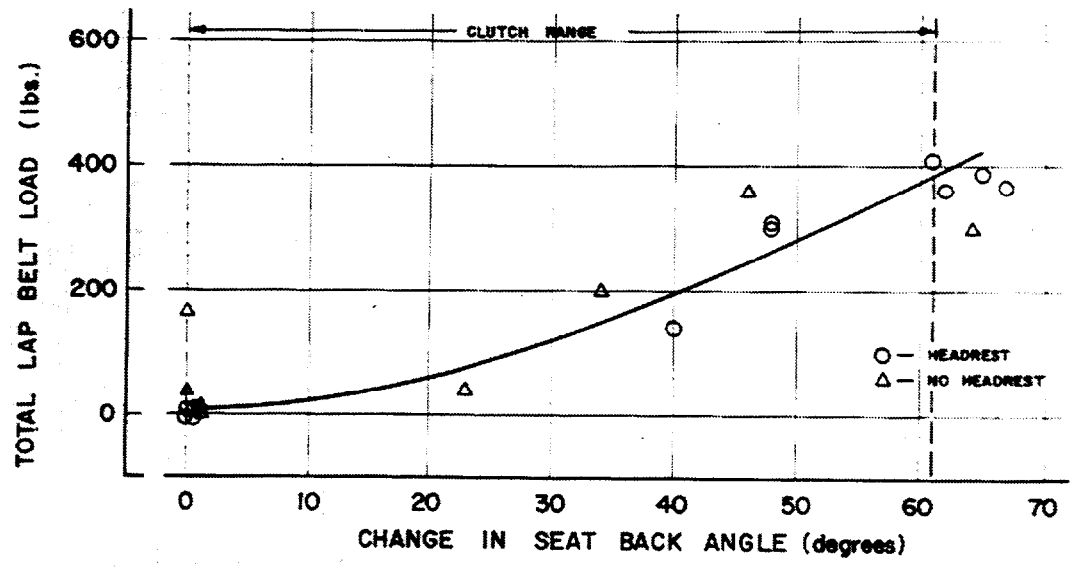
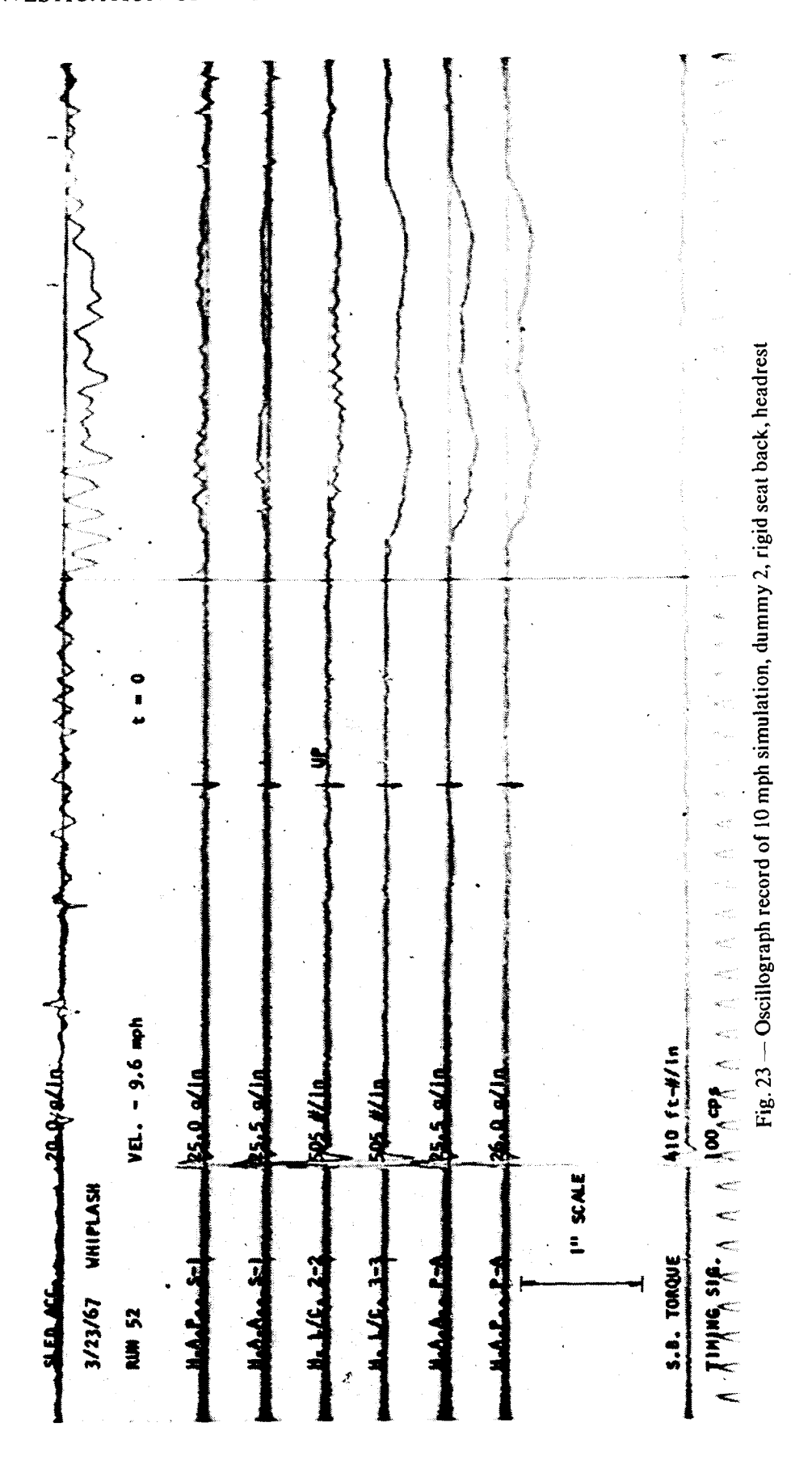
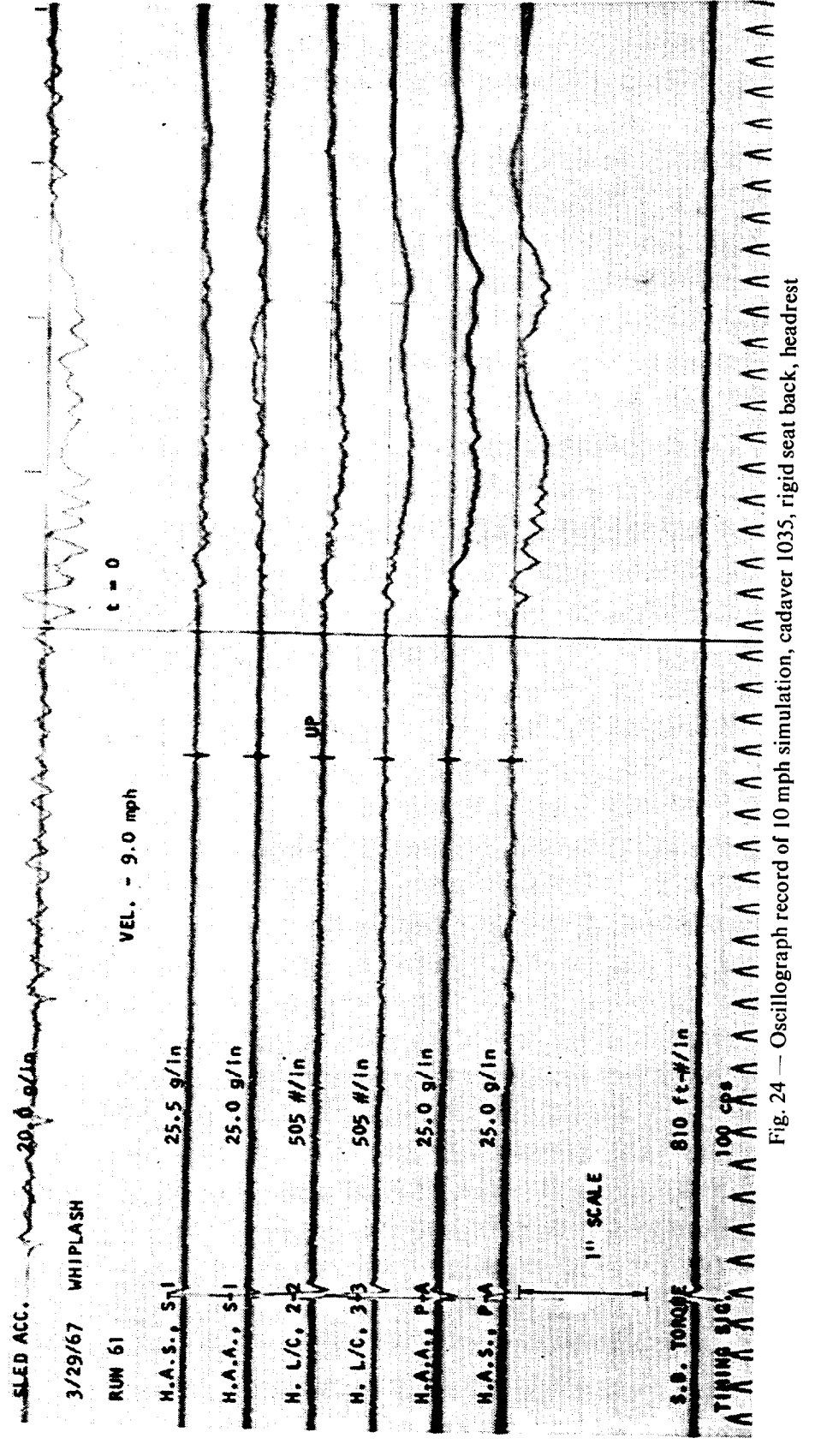
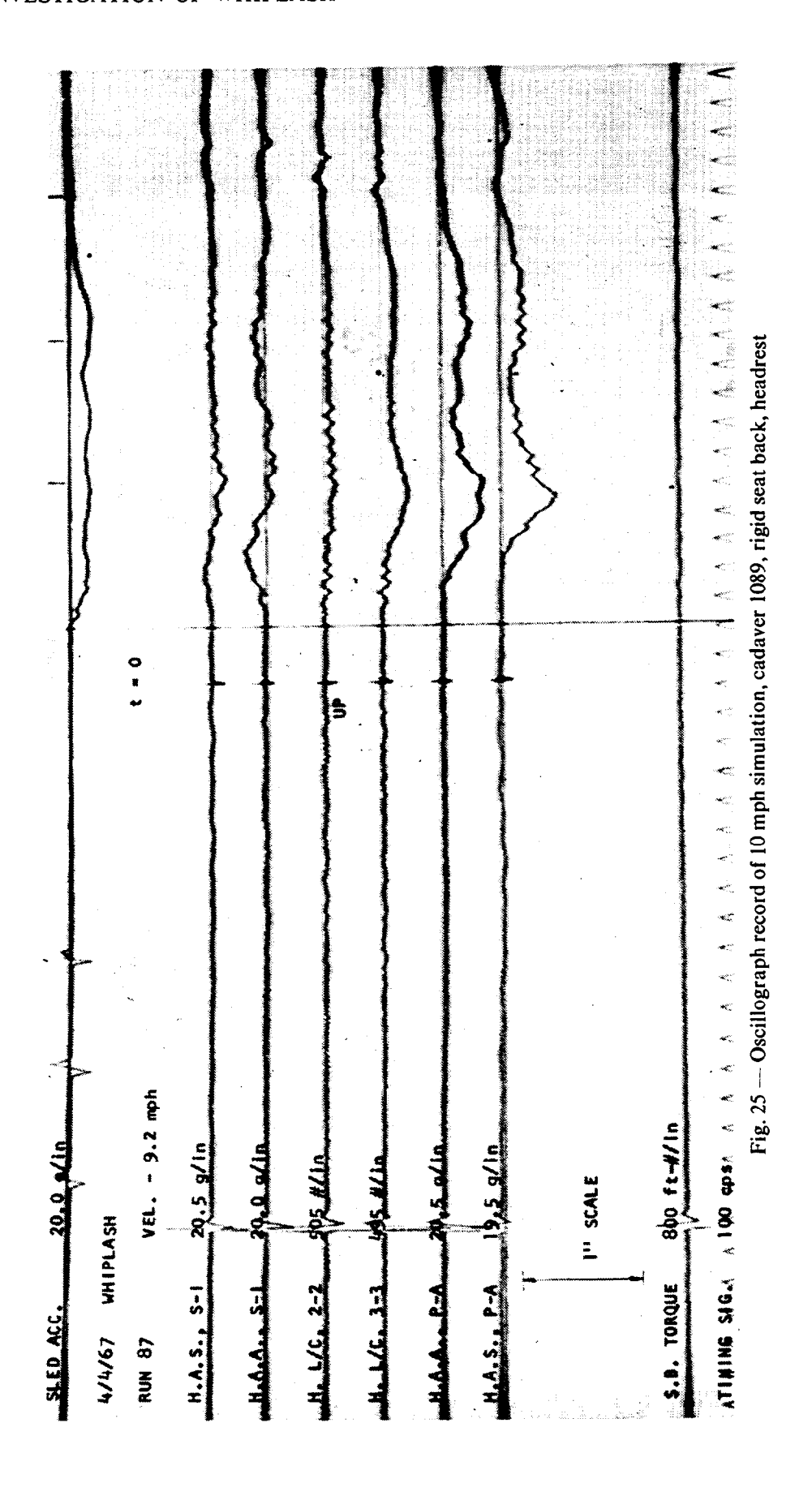
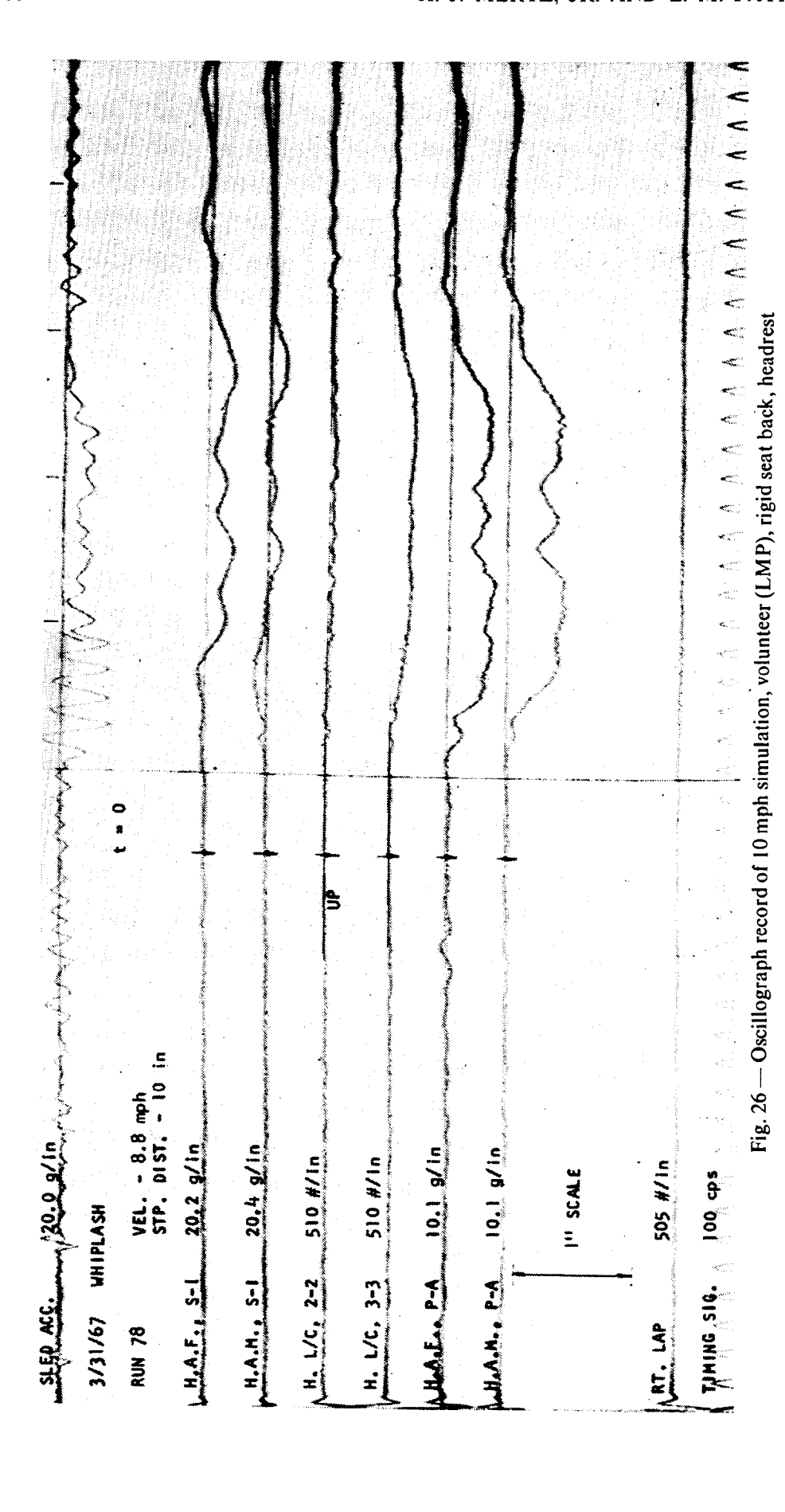


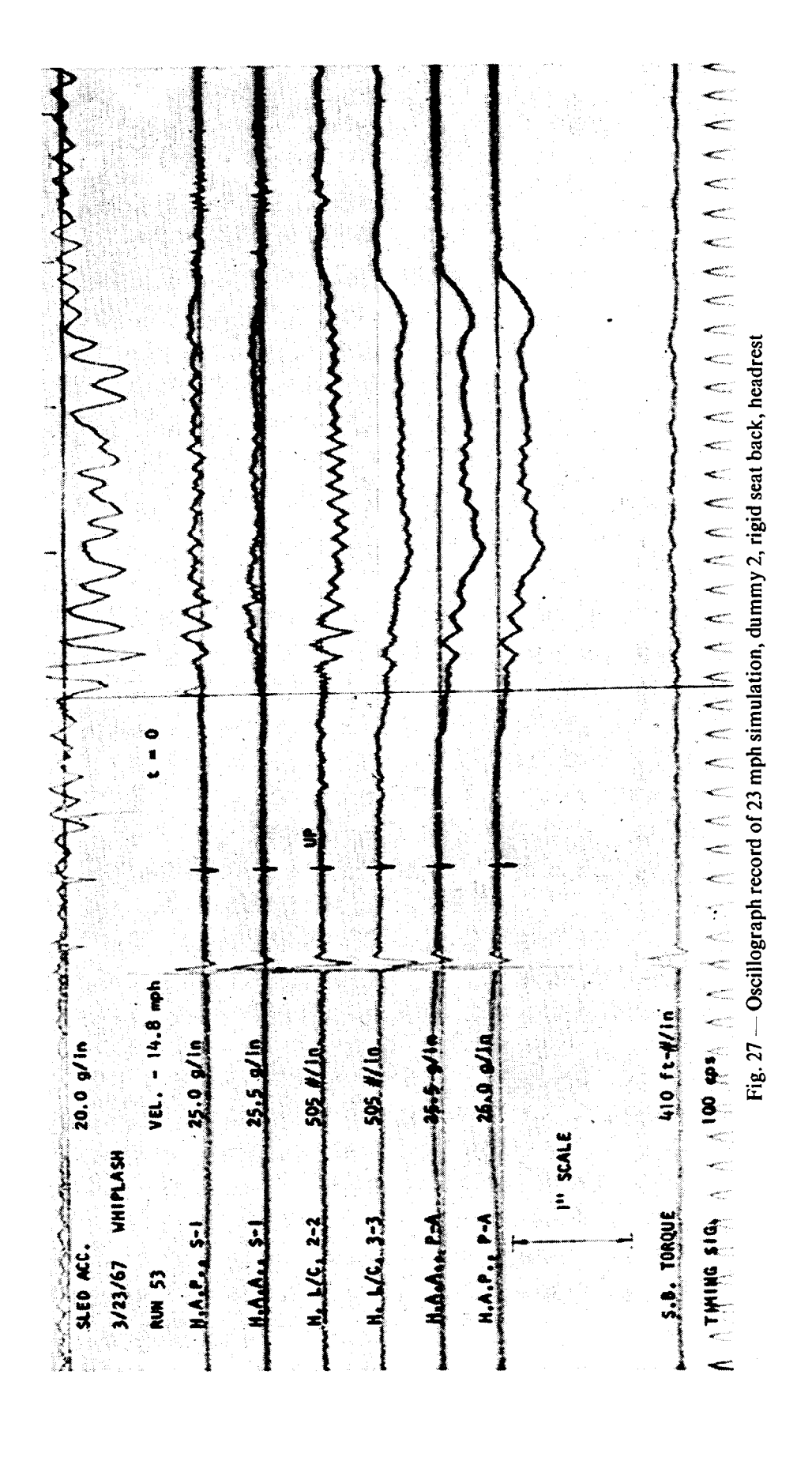
Fig. 22 - Maximum lap belt load on subject as related to maximum change in seat back angle











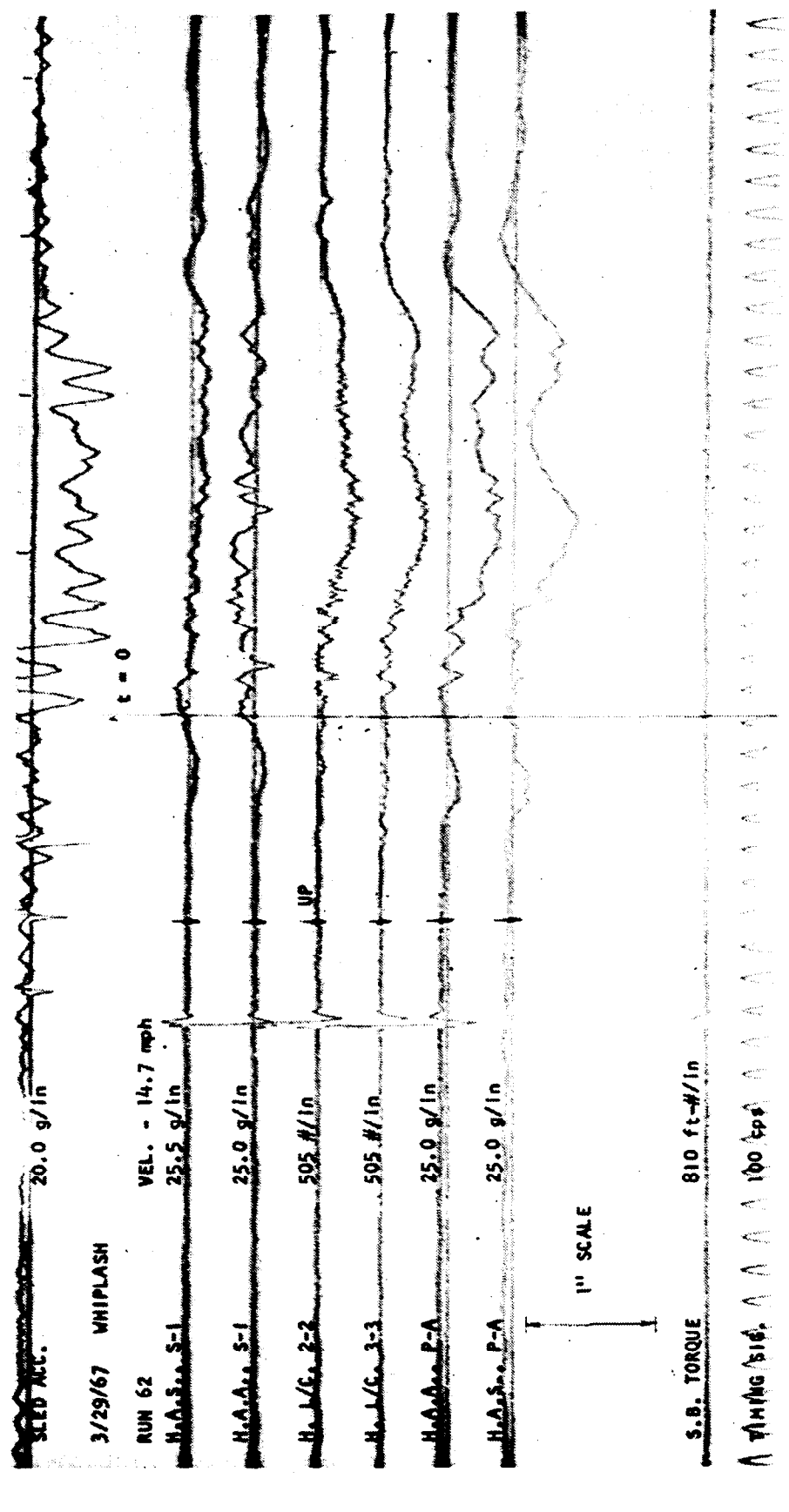
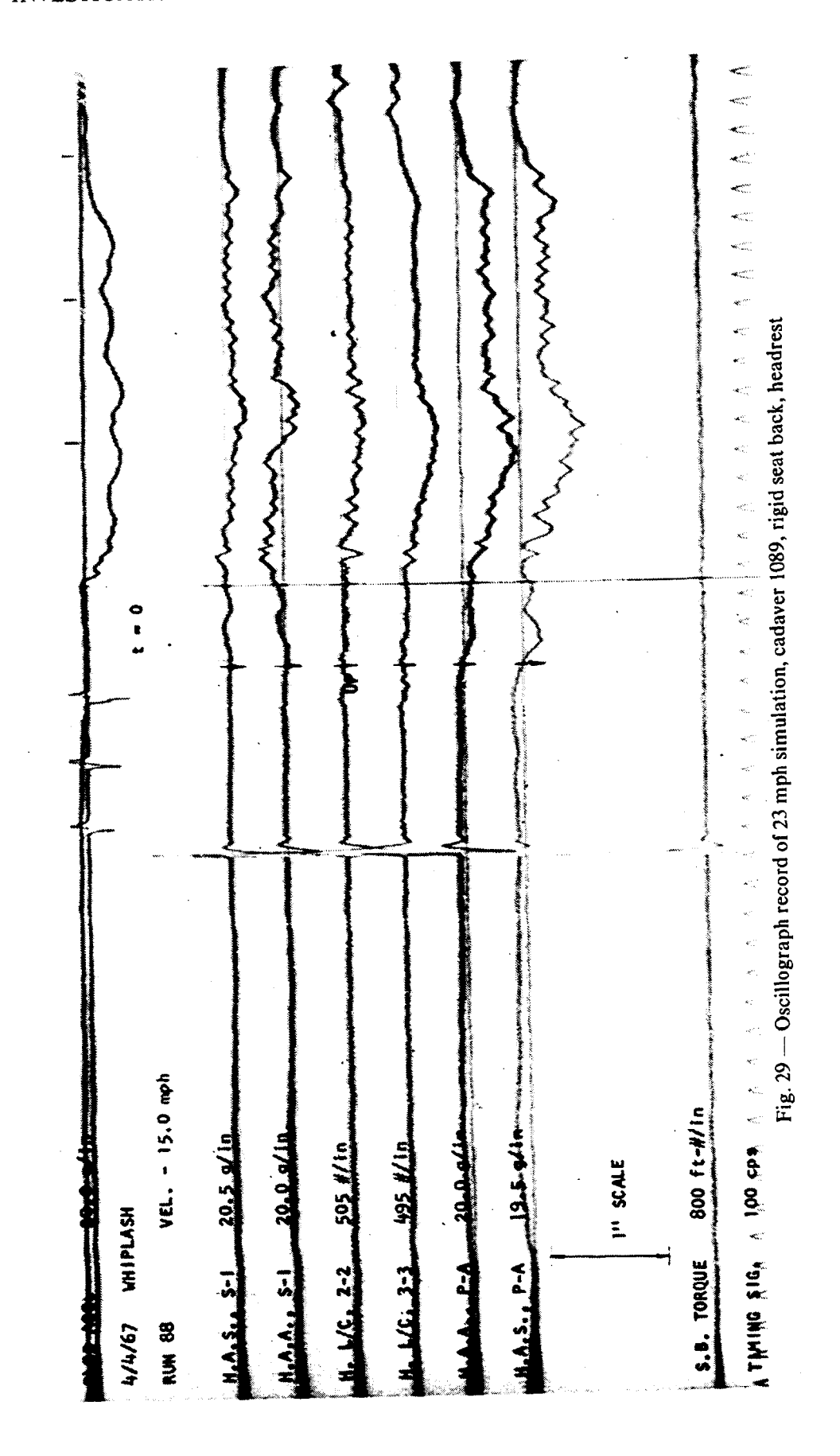


Fig. 28 — Oscillograph record of 23 mph simulation, cadaver 1035, rigid seat back, headrest



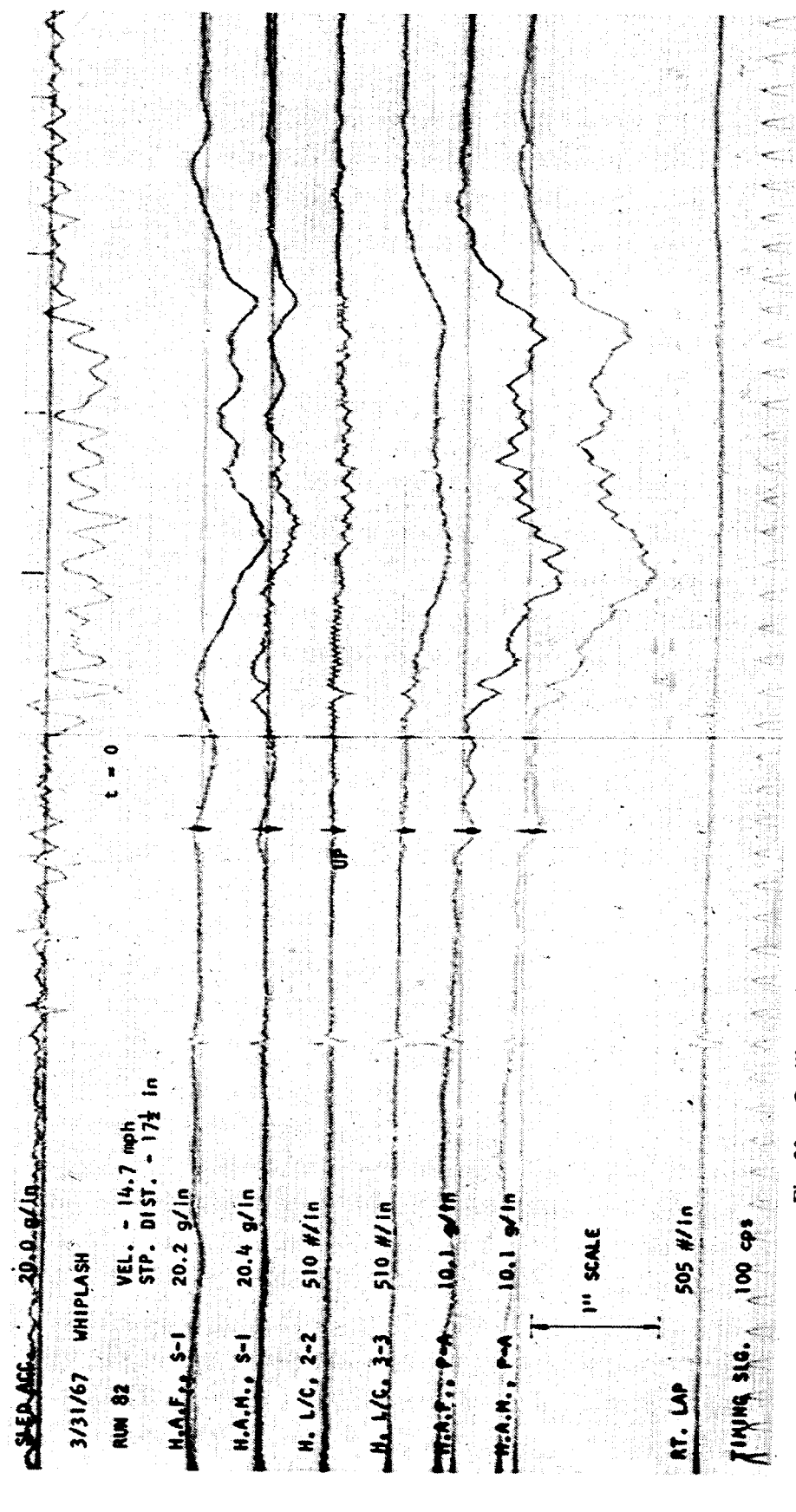


Fig. 30 — Oscillograph record of 23 mph simulation, volunteer (LMP), rigid seat back, headrest

on the head, the corresponding neck torques were not computed. However, the neck torque and the axial force are not critical parameters when a flat headrest is used, since there is very little head rotation and the principal head load is approximately normal to the axial direction.

A comparison of the maximum shear forces for the various subjects is shown in Fig. 32. For the 10 mph simulation the correlation between the different subjects is good, but for the 23 mph simulation the shear force values of 132 and 107 lb for cadavers 1035 and 1089 are greater than the shear values of 70 and 59 lb for the volunteer and dummy 2. However, the magnitude of the shear load depends on the point of application of the headrest load on the head and, consequently, fluctuation should be expected between subjects. In any case, all the shear loads are below the static voluntary tolerance level of 190 lb.

Human Voluntary Simulations with Headrest - For these simulations the volunteer was lap belted, his head was initially in contact with the flat surface of the load cell which was padded with one layer of 5/8 in. thick Rubatex, and the seat back was held

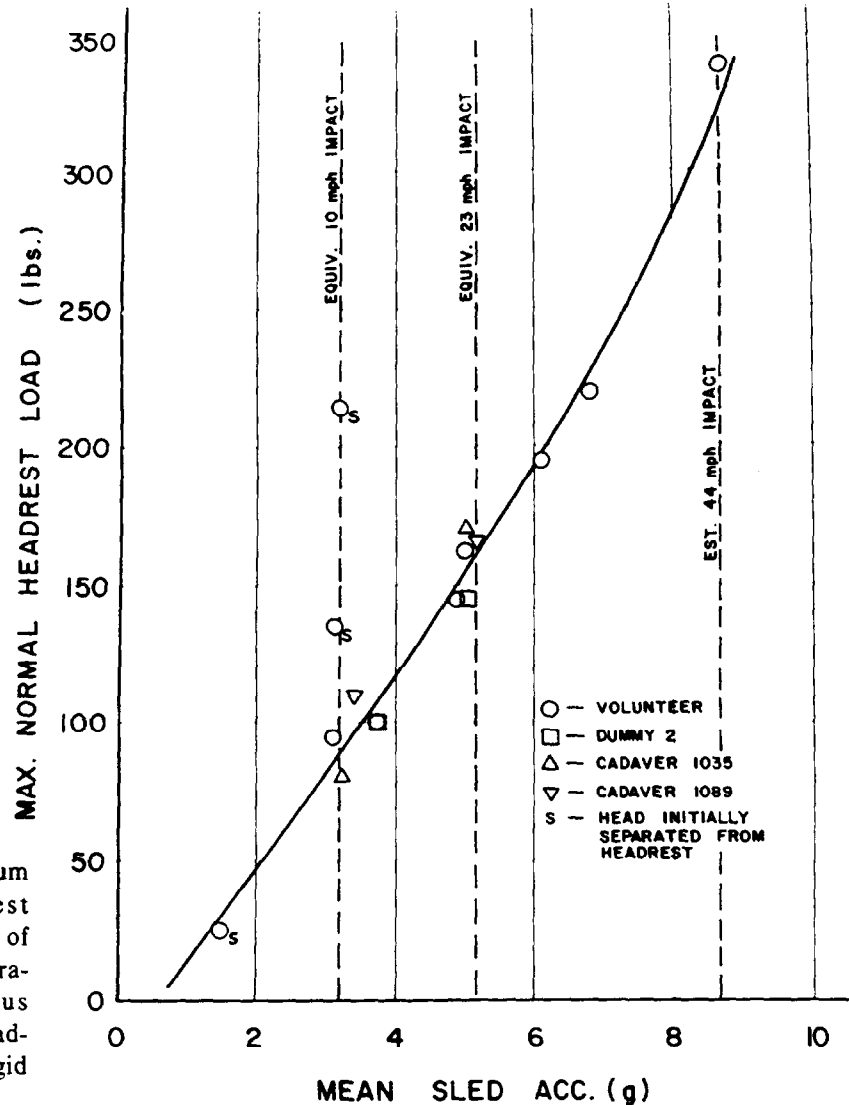


Fig. 31 — Maximum normal headrest loads as function of mean sled acceleration for various subjects, flat headrest, belted, rigid seat back

rigid. The volunteer was subjected to various constant acceleration pulse levels with the maximum being 8.65 g. The curves on Figs. 31 and 32 depict the maximum normal headrest loads and the corresponding maximum shear loads, respectively, which the volunteer withstood during these various mean sled acceleration levels.

The curve is linear because the head which is initially in contact with the headrest undergoes a pure translational motion which is identical to the sled's motion. Consequently, for this configuration the headrest load must be directly proportional to the sled acceleration. This dependence on sled acceleration can be demonstrated further by considering the two points on Fig. 31 which represent the responses of the volunteer for an equivalent 23 mph rear-end collision. The headrest loads of 145 and 162 lb were achieved using initial sled velocities of 11.0 and 14.7 mph with corresponding stopping distances of 10 and 17.5 in., which upon applying the relationships for constant accelerations gave approximately the same mean sled accelerations of 4.85 and 4.95 g, respectively.

The maximum mean sled acceleration which the volunteer was subjected to was 8.65 g and only because of fatigue did he stop at this level. The corresponding maximum normal headrest and neck shear loads were 340 and 150 lb, respectively.

To estimate an equivalent rear-end impact at this mean acceleration level, the equivalent car impact velocities of 0, 10 and 23 mph were plotted as a function of mean acceleration as shown in Fig. 33. Since this curve has an increasing slope, a conservative extrapolation can be obtained by extending the chord for the 10 and 23 mph impacts until it intersects the line for 8.65 g which gives a corresponding

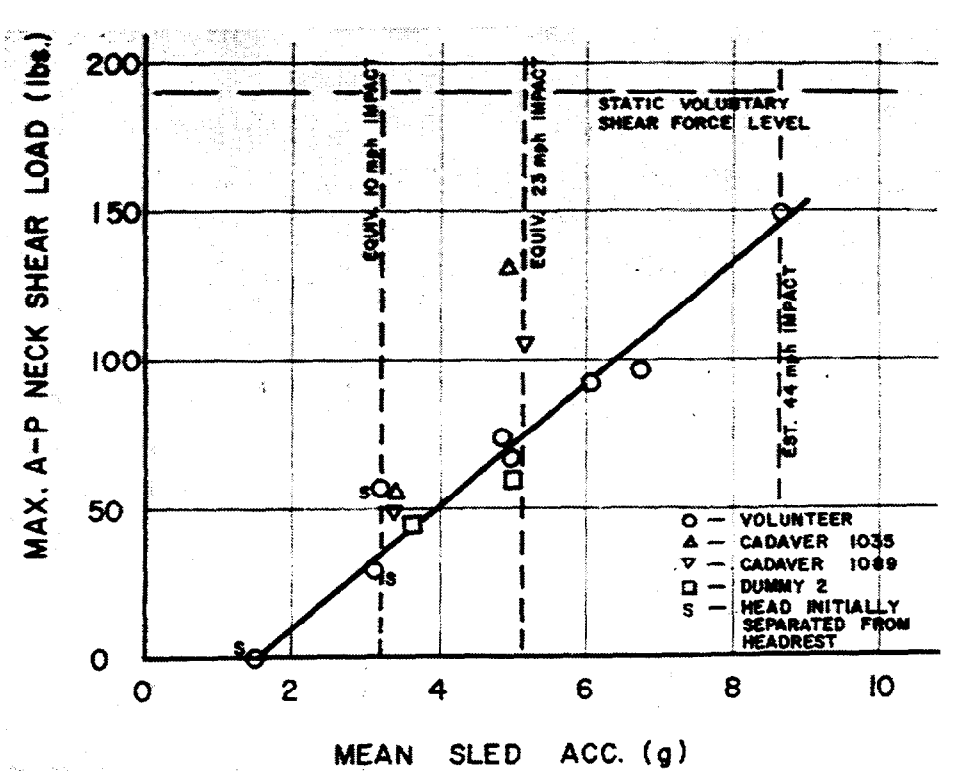


Fig. 32 — Maximum A-P neck shear forces as function of mean sled acceleration for various subjects, flat headrest, belted, rigid seat back

equivalent car impact velocity of 44 mph. As a further check on this approximation the change in velocity of the struck car (the simulation velocity for the sled) is also plotted as a function of the mean acceleration. A linear relationship exists between the change in velocity of the struck car and its corresponding mean acceleration because the differences in pulse time between the two impact conditions (9 and 15 mph changes in velocity) were small when compared to the total pulse duration. Extending this line to 8.65 g gives a change in velocity of the struck car of 25 mph. Since the approximations for the 10 and 23 mph simulations were obtained from impacts between cars of equivalent weights in which no braking action was used, these approximations also applied for this estimation. Consequently, the law of conservation of linear momentum is valid under these conditions and the final velocity of the striking car for any initial velocity can be approximated directly by taking the differences of the ordinates of the two curves for the prescribed impact velocity. Knowing the initial and final velocity of both cars, the coefficient of restitution can be calculated from

$$e = \frac{(u_1 - u_2)}{(v_2 - v_1)}$$

where: u_1 and $u_2 = V$ elocities of the striking and struck cars after impact v_1 and $v_2 = V$ elocities before impact, respectively

For a perfectly elastic impact e = 1 and for a perfectly plastic impact e = 0.

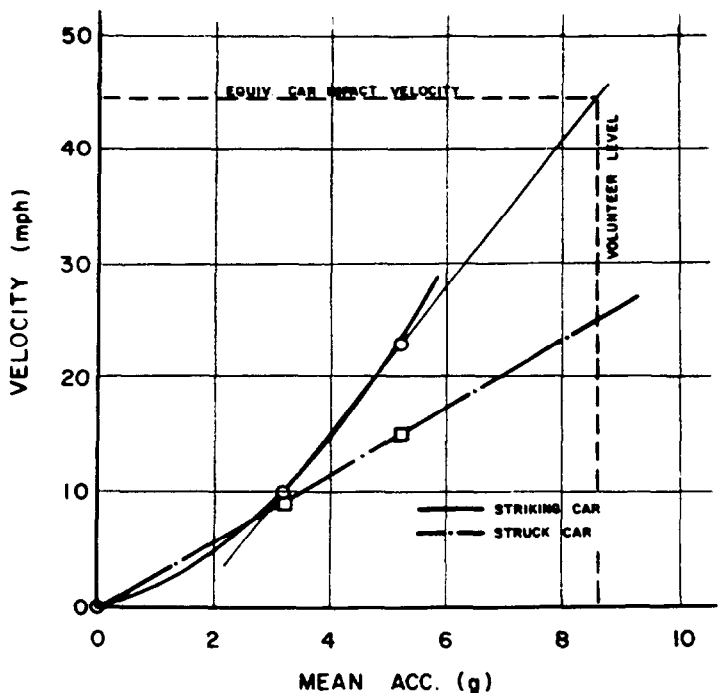


Fig. 33 — Estimation of relative impact velocity of cars of equal weight involved in rear-end collision based on mean car frame acceleration

As the initial relative velocity between impacting cars increases, the percentage of plastic to elastic deformation should increase and this trend will be reflected in a decrease in the coefficient of restitution. The estimated 44 mph rear-end collision fits into this tendency as illustrated by the values of the coefficient of restitution, 0.80, 0.30, and 0.14, for the 10, 23 and 44 mph equivalent rear-end collisions, respectively.

The 44 mph simulation was achieved using a sled velocity of 14.7 mph instead of the 25 mph which is indicated by the change in velocity for the struck car given in Fig. 33. However, as demonstrated previously, the important parameter in the case where the head is initially in contact with the headrest is the mean acceleration. Consequently, the simulation condition which gives a mean sled acceleration of 8.65 g does duplicate the loading during a 44 mph rear-end collision with the only difference being that the pulse duration for the 14.7 mph simulation will be less than for the 25 mph simulation. However, in either case the duration would be classified as "long" (> 100 ms) and have no effect on the volunteer's response to either simulation. Based on these assumptions, it is physically possible for a person to withstand a 44 mph rear-end collision with no injuries, provided his head is initially in contact with a flat headrest which is firmly attached to a rigid seat back.

It should be emphasized that this statement is for a flat headrest. Using a curved headrest, the relative position of the head with respect to the headrest at contact determines the point of application of the applied load. If the load is applied above the

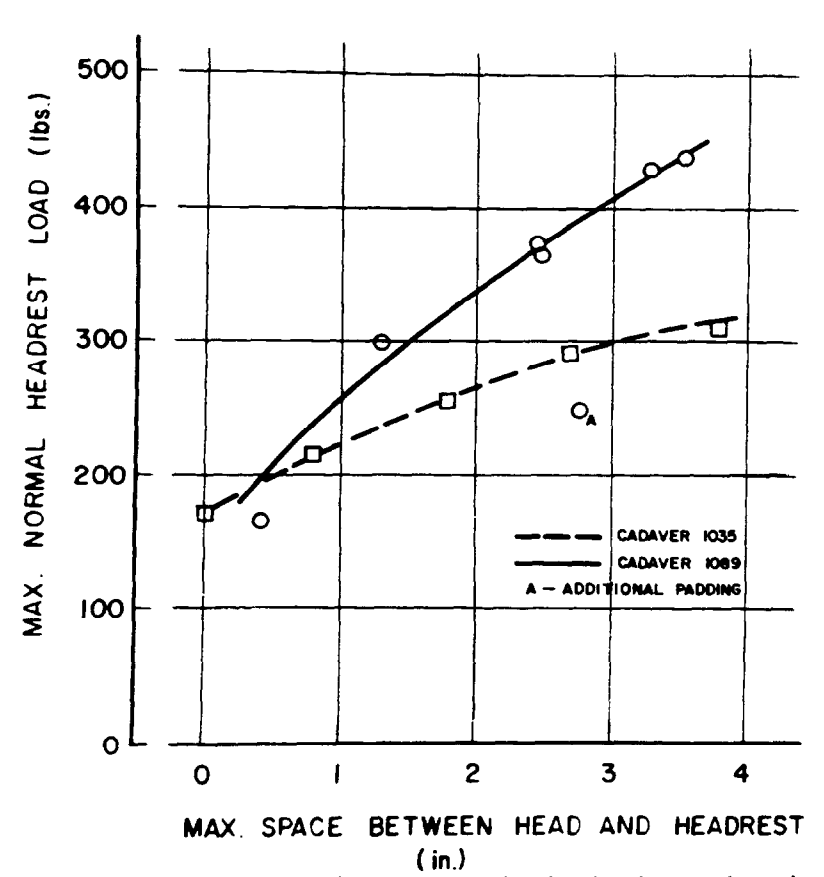


Fig. 34 — Relationship between the relative position of head to headrest and maximum normal headrest load, 23 mph simulation, rigid seat back, flat headrest, lap belted

c.g. of the head, flexion of the neck will occur, and if the headrest is in the neck area, extension of the neck will occur. Neither of these conditions was evaluated with the volunteer.

Effect of Initial Separation of Head with Respect to Headrest - In two instances for the equivalent 10 mph impact, the volunteer's head was not initially in contact with the headrest. The result was that the maximum headrest loads were greater (215 and 135 lb as compared to 90 lb) than when his head was initially in contact. To evaluate this effect, both cadavers were subjected to a sequence of 23 mph simulations identical in setup to the comparison runs, except the distance between the head and the headrest was incrementally increased. The results of these simulations are shown in Fig. 34. For cadavers 1089 and 1035 the normal headrest loads corresponding to a 3-1/2 in. separation were 440 and 310 lb, respectively, compared to approximately 150 and 170 lb for no separation. However, by taping a piece of 1-1/8 in. styrofoam to the back of the head of cadaver 1089, the headrest load for a separation of 2-3/4 in. as indicated by the point with the subscript in Fig. 34 was reduced from 390 to 250 lb.

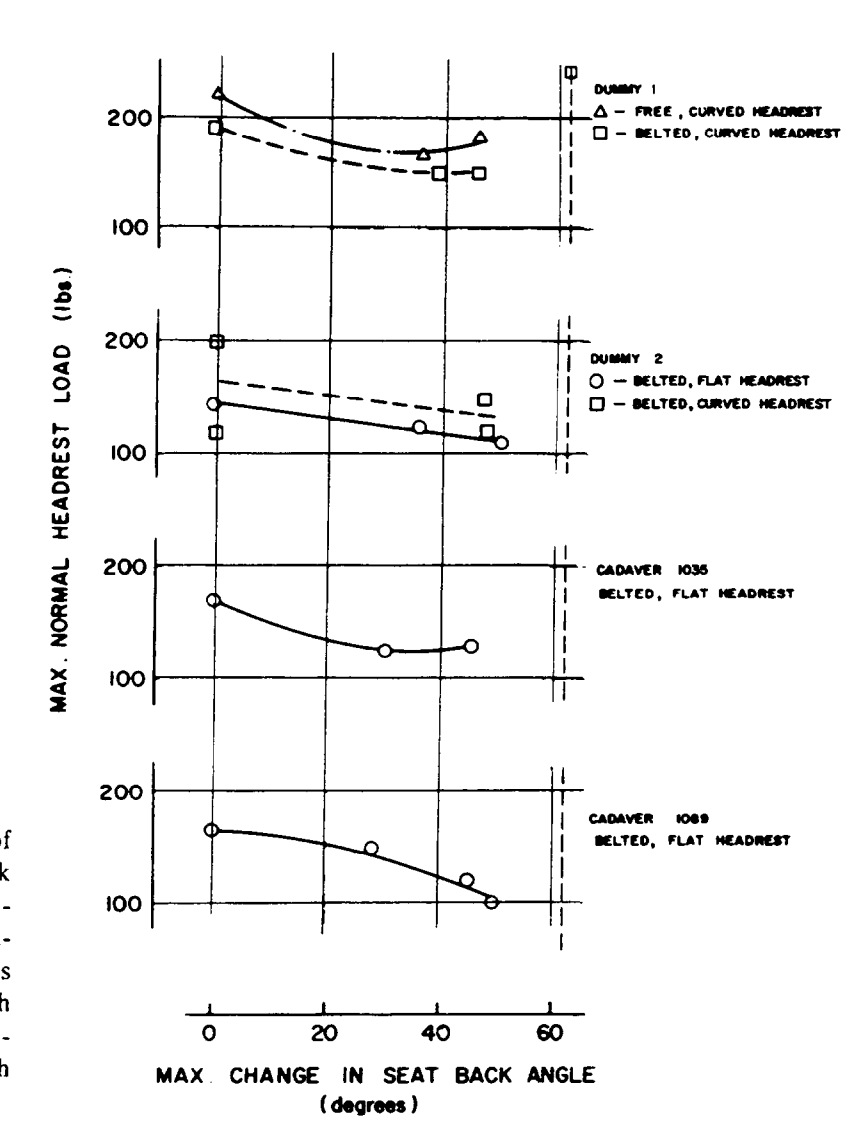


Fig. 35 — Effect of degree of seat back rotation on maximum normal headrest loads for various subjects, 23 mph simulation, head initially in contact with headrest

Consequently, with adequate padding and proper design of the headrest supporting structure, headrest loads for any given head separation can be attenuated with the minimum load for any given mean acceleration being given by the condition of no initial separation.

Effect of Seat Back Rigidity on Maximum Normal Headrest Load - For these simulations the equivalent 23 mph rear-end collision was used and the subject's head was initially in contact with the headrest. Fig. 35 depicts the effect that seat back rotation has on the resulting maximum normal headrest load.

For dummy 1 only a curved headrest was used and the simulations were conducted with the subject free and lap belted. The response of the dummy with these two types of restraint are quite similar with head loads being approximately 25 lb higher when the dummy is unrestrained.

The relatively large load of 245 lb, which occurred for the lap belted case for a change in angle of 62 deg, resulted because the seat back "bottomed" on mechanical stops which produced an incremental change in the relative velocity between the head and the headrest, resulting in an equivalent impact loading even though the head was in contact with the headrest.

For dummy 2 both a curved and flat headrest were used. The data using the curved headrest are quite scattered compared to response of the dummy using a flat headrest. In general for all subjects, the headrest load decreased as the seat back rigidity decreased which implies that seat back rotation tends to reduce the severity of a given rear-end collision, as was the case for the unsupported head. However, a practical limitation must be placed on the degree of rotation because the driver of the struck car must be in a position to regain control of his car after the collision.

Conclusions

- 1. In the case where the car is not equipped with headrests, tensing of neck muscles prior to the impact reduces the possibility of neck injury. The severity of a rear-end collision can be reduced further by flexing the head forward and preventing extension by clasping the hands behind the head.
- 2. With or without a headrest, controlled seat back collapse reduces the severity of impact. Further study is needed to determine if there is an optimum rotational characteristic.
- 3. For the unsupported head simulations, cadavers give good representation of the responses of people who are not expecting the rear-end impact. Neither dummy used gave satisfactory responses.
- 4. With the head initially in contact with the headrest, the responses of all subjects were closely related.
- 5. With initial separation between the head and the headrest, head loads are higher than with no initial separation. With adequate padding and proper structural design of the headrest, the head loads can be reduced.
- 6. With the head in contact with a flat headrest and the seat back rigid, a 44 mph rear-end collision can be withstood with little discomfort.
- 7. Because of the low energy-storing characteristics of the seat used, no appreciable head flexion due to rebound occurred for any of the configurations evaluated.

- 8. Neck torque at the occipital condyles is the limiting factor in neck injury rather than the shear or axial forces.
- 9. Results using a curved headrest were scattered. Further evaluation of positioning and optimum curvature of the headrest is needed.
- 10. The type of restraint (lap belted, lap and diagonal chest belted, or free) had little effect on the response of the subject when the seat back was rigid.
- 11. With seat back rotation, the lap belt was loaded and increased the severity of the impact in the unsupported head case and had no effect when the head was supported.
- 12. The diagonal chest strap did not provide any restraint for the configurations in which it was used.
- 13. Responses of subjects to various degrees of severity of rear-end collisions can be compared on the basis of an index based on the static, voluntary, extended head, neck torque tolerance level with a preliminary tolerable index of 2.00 being given. This value may be changed as further data become available.

Acknowledgments

The authors wish to express their gratitude to Dr. I.D. Harris for providing the radiological diagnoses of the cadavers, to Clarence Murton for his help in conducting the simulations, and to the members of the Biomechanics Staff of the Engineering Mechanics Department of Wayne State University who contributed to this project.

Also, the services of the Computing and Data Processing Center of Wayne State University for providing the computer time needed for the numerical analysis are gratefully acknowledged.

References

- 1. D.M. Severy and J.H. Mathewson, "Automobile Barrier and Rear-End Collison Performance." Paper 62C presented at SAE Summer Meeting, Atlantic City, June 1958.
- 2. J.P. Stapp, "Medical Aspects of Safety Seat Belt Development." Proceedings of Sixth Stapp Car Crash and Field Demonstration Conference, 1963.
- 3. D.F. Carroll, J.A. Collins, J.L. Haley, Jr., and J.W. Turnbow, "Crashworthiness Study for Passenger Seat Design Analysis and Testing of Aircraft Seats." AvSER 67-4, May 1967.
- 4. Carroll F. Simmons and David N. Herting, "Strength of the Human Neck." Life Sciences Department, Space and Information Systems Division, North American Aviation, Inc., SID 65-1180, Sept. 22, 1965.
- 5. K.N. Naab, "Measurement of Detailed Inertial Properties and Dimensions of a 50th Percentile Anthropometric Dummy." Proceedings of 10th Stapp Car Crash Conference, 1966.
- 6. W.T. Dempster and G.R.L. Gaughran, "Properties of Body Segments Based on Size and Weight." The American Jrl. of Anatomy, Vol. 120, No. 1, January, 1967.
- 7. John Martinez, J. Wickstrom, and B. Barcelo, "The Whiplash Injury A Study of Head-Neck Action and Injuries in Animals." Paper 65-WA/HUF-6, presented at ASME meeting, Chicago, November 1965.